UNIVERSITÀ DEGLI STUDI DI PADOVA

DIPARTIMENTO DI INGEGNERIA INDUSTRIALE

CORSO DI LAUREA MAGISTRALE IN INGEGNERIA CHIMICA E DEI PROCESSI INDUSTRIALI

Tesi di Laurea Magistrale in
Ingegneria Chimica e dei Processi Industriali

Synthesis, optimization and 3D bioprinting of gelatin methacrylate hydrogels for cell culture studies

Relatore: Prof.ssa Elisa Cimetta

Correlatore: Dott. Lorenzo Bova

Laureando: MARCO MANTOVANI

ANNO ACCADEMICO 2018 – 2019

Riassunto

La stampa 3D è un processo che permette la creazione di strutture complesse a partire da materie prime e processi relativamente semplici. Se impiegata nel settore biomedico, ad esempio nella modellazione del cancro o nell'ingegneria tissutale, si parla allora di biostampa 3D, un processo in costante via di sviluppo e dotato di enormi potenzialità per lo studio dei tumori.
La biostampa 3D infatti sfrutta la combinazione di biomateriali e cellule per creare strutture con lo scopo di rappresentare in maniera fedele i tessuti naturali o gli organi.
Pertanto, l'obiettivo di questa Tesi sono lo studio e l'ottimizzazione di un hydrogel a base di gelatina metacrilata (GelMA), un polimero sintetizzato modificando la struttura di un materiale con origine naturale come la gelatina, e l'analisi del comportamento cellulare all'interno di strutture 3D ottenute attraverso biostampa di questo materiale.
Una volta formato l'hydrogel, si analizzeranno la vitalità e la migrazione delle cellule all'interno di esso; l'applicazione finale porterà allo studio in hydrogel anche degli esosomi derivati dal Neuroblastoma, per comprendere il ruolo che queste vescicole extracellulari hanno nella proliferazione delle metastasi di questo tumore.
Nella fase iniziale, sono state ottimizzate la sintesi della gelatina metacrilata e la produzione dell'hydrogel; successivamente è stata utilizzata la modellazione 3D per la progettazione delle strutture oggetto di stampa.
Il polimero e l'hydrogel utilizzati sono stati sottoposti ad alcuni test per ricavarne informazioni riguardanti le loro temperature caratteristiche, la viscosità dell'hydrogel e la sua proprietà di rigonfiamento, fattore molto importante che è correlato fortemente alla concentrazione di polimero nell'hydrogel.
Nella validazione biologica dell'hydrogel sono state utilizzate due linee cellulari: cellule renali embrionali e cellule di Neuroblastoma. Queste, dopo essere state coltivate all'interno delle strutture in 3D, sono state analizzate mediante una soluzione contenente diversi marcatori fluorescenti. Ciò ha permesso di verificare non solo la vitalità cellulare all'interno dell'hydrogel, ma anche osservare l'eventuale migrazione spontanea al suo interno.
Infine, le cellule di Neuroblastoma umano sono state seminate nell'hydrogel e biostampate in presenza anche degli esosomi, al fine di studiarne la loro migrazione e internalizzazione all'interno delle cellule.

Summary

3D printing is a process that allows the creation of complex structures starting from relatively simple raw materials and procedures. If used in the biomedical field, for example in cancer modeling or in tissue engineering, it's defined as 3D bioprinting, a process in constant development and with an enormous potential for tumor studies.
3D bioprinting uses a combination of biomaterials and cells to create structures with the aim of faithfully representing natural tissues or organs.
Therefore, the objective of this thesis are the study, characterization and optimization of a hydrogel based on gelatin methacrylate (GelMA), a polymer synthesized by modifying the structure of a material with natural origin such as gelatin, and the analysis of cellular behavior within hydrogel-based 3D printed structures.
Once the hydrogel is formed, the viability and migration of cells within it will be analyzed; the final application will also lead to adding Neuroblastoma-derived exosomes to the hydrogel, to understand the role these extracellular vesicles play in the metastatic dissemination in this type of cancer.
In the initial phase, the synthesis of gelatin methacrylate and the production of the hydrogel were optimized; then 3D modeling was used for the design of the structures to be printed.
The polymer and hydrogel used were subjected to some tests to obtain information regarding their characteristic temperatures, the viscosity of the hydrogel and its swelling property, a very important factor that is strongly related to the polymer concentration in the hydrogel.
Two cell lines were used in the biological validation of the hydrogel: embryonic kidney and neuroblastoma cells. These, after being cultivated inside the 3D structures, were analyzed using a solution containing different fluorescent markers. This allowed to verify not only the cellular viability within the hydrogel, but also to observe the possible spontaneous migration within it.
Finally, human Neuroblastoma cells were seeded in the hydrogel and bioprinted in the presence of exosomes, in order to study their migration and internalization within the cells.

Table of contents

List of Figures

List of Tables

Introduction

3D bioprinting is a powerful and relatively well-established technology that allows the use of bioinks as biocompatible materials for the construction of three-dimensional structures capable of representing the complexity of the environment in which cells live naturally. An ideal bioink, such as a hydrogel, should have some features including excellent bioprintability, high mechanical integrity, biocompatibility and non-toxicity. For these reasons, this technology is widely used in biological and biomedical applications.

The laboratory where this thesis work was performed, BIAMET (*Biomedical Applications of Multiscale Engineering Technologies*), is a laboratory where biology, engineering, medicine and biotechnology meet together to study human cancer disease, and Neuroblastoma in particular. In this laboratory, the tools mainly used to reach these results are a 3D bioprinter and microfluidic platforms, which have to be constantly developed and improved to keep up with the new technologies.

In the last twenty years, the use of 3D bioprinting has had a great impact on biological applications; this is due to the fact that, inside the human body, cells reside in a complex 3D extracellular matrix (ECM), so traditional 2D *in vitro* cell culture studies have inevitable limitations. Biological processes such as cancer development, cancer metastasis, and embryogenesis depend a lot on cellular mechanotransduction, cell-cell and cell-ECM interactions and cell migration.

There are three main 3D bioprinting technologies, which exploit hydrogels as bioinks which, thanks to their large amount of liquid content, are highly biocompatible materials.

An advantage in the use of hydrogels consists in the possibility of adjusting their mechanical properties, the properties related to degradation, and the level of hydration of the matrix; all these features can be modulated in order to obtain materials with similar properties to those of human tissues, thus being able to use them in specific biological applications.

The aim of this thesis consists in the design and development of a gelatin methacrylate-based cell-laden hydrogel capable of representing the natural ECM in order to study the cell viability and migration within it and the role of exosomes in the metastatic dissemination of Neuroblastoma cancer (NB).

Neuroblastoma is a childhood solid tumor originating from progenitor cells of the sympathetic nervous system. Metastases are found in approximately half of NB patients, primarily located in bone, bone marrow, lymph nodes, liver and skin. The complex molecular mechanisms that are involved in cancer dissemination are not completely understood, because of the lack of appropriate means to study them. Exosomes are vesicle-like structures that are normally secreted by cells. They range in size between 50 and 100 nm and their content (cargo) is a

known regulator of cell-cell communication. Several studies have demonstrated that exosomes deliver signals that promote tumor progression, invasion and metastasis both locally and at distant recipient sites.

The structure of the thesis is as follows.

In the first chapter some general notions about the importance of a three-dimensional cell culture and 3D bioprinting will be introduced, also focusing on materials commonly used in this type of technique. The chapter includes also a description of Neuroblastoma and the role of exosomes in the dissemination of this type of cancer.

The second chapter describes the procedures and protocols followed during the activity, starting from the synthesis of the polymer, followed by the preparation and optimization of the gelatin methacrylate hydrogel. Subsequently, in order to obtain a characterization of the materials used, the mechanical tests carried out on the hydrogel and polymer are explained. The choice of the structures used for the 3D bioprinting will then be analyzed and what concerns the performed cellular tests is introduced.

In the third chapter the improvements obtained regarding the optimization of gelatin methacrylate synthesis and the hydrogel preparation are exposed; the experimental results from the mechanical and cellular tests are then explained. First of all, HEK-293 cell lines are used for a viability test and to evaluate the hydrogel biocompatibility. After that, a specific Neuroblastoma cellular line of SK-N-AS is tested for a more thorough biological validation.

For sake of completion, the Appendix collects information on all remaining experiments that did not result in the successful obtainment of relevant biological data.

Chapter 1

State of the art

In this chapter some general notions about the importance of a three-dimensional cell culture and 3D bioprinting will be introduced, also focusing on materials commonly used in this type of technique.

1.1 3D cell culture

From the analysis of the structure of biological organs and tissues, it is possible to extract important clues to help us design a biomimetic matrix relevant for *in vitro* imitation of the natural extracellular matrix (ECM). Human tissues are made up of sequences of three-dimensional repetitive units with an order of magnitude of thousands of micrometers: cells reside inside these structures, interacting with the ECM and among themselves [(1)].

Although several studies have already shown that a two-dimensional cell culture fails to fully represent the natural dynamics of cells [(2)], 2D cell cultures are still widely used in biological studies even with their inevitable limitations. In order to improve these applications, it's crucial to develop techniques that allow to obtain *in vitro* models more faithful to the physiological three-dimensional distribution of cell populations. Cell culture in structures spatially faithful to *in vivo* patterns can achieve an excellent representation of the complexity of the environment where cells naturally live, in which spatial interactions between the different cells also play an important role [(3)].

Furthermore, two-dimensional cultures polarize cells in such a way that most of their surface is exposed to the culture medium, while only a small part is in contact with the other cells; this behavior induces unnatural mechano-transduction mechanisms.

However, *in vivo* there is a dynamic spatial gradient of the elements that influence migration and cell-cell interaction [(4)]. It follows that in order to achieve an adequate *in vitro* reproduction of cell life and mechano-transduction processes, cells should be cultivated in 3D microenvironments, so as to best represent the critical mechanical factors typical of the natural ECM, which in a 2D culture cannot be reproduced, as can be seen in Figure 1.1.

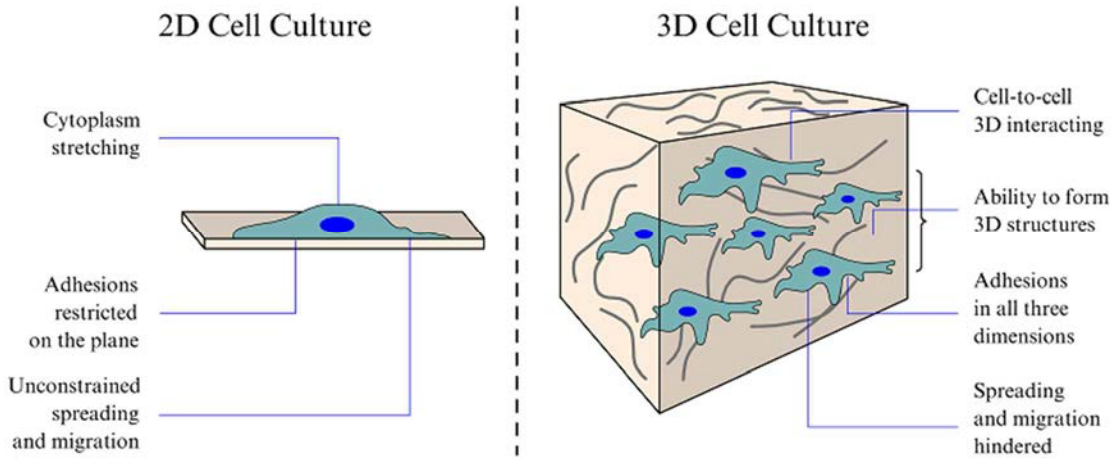

Figure 1.1 *Comparison between 2D cell culture and 3D cell culture showing the main differences between cells behavior and constraints when cultivated in 2D environment* [5].

1.1.1 Mechanotransduction

Cellular mechanotransduction is the molecular mechanism through which cells sense a mechanical stress and respond to it.

Numerous studies on a wide range of diseases belonging to any field of medicine investigate the causes that induce these phenomena, demonstrating that many of these have a common peculiarity, namely that their clinical presentation has a derivation from an abnormal mechanotransduction. More and more evidence has been found that the stiffness of the ECM regulates the function and mechanics of cancer cells, influencing the typical characteristics of the disease as metastasis and migration [6,7].

The stiffness of the tissue is strictly regulated under normal conditions, but this changes in disease states. In cancer, tumors are almost always more rigid than the surrounding non-involved tissue, even if the cells soften [8].

By exploiting variations in the structure of the extracellular matrix, changes in mechanics of cells, or by altering the molecular mechanisms by which cells convert the mechanical signals received, it is possible to deeply modify the cytoskeletal response and, thus, the genetic expression of cells [9]. In this way, it could be possible to use this knowledge to therapeutically intervene on the molecules that regulate mechanotransduction, including extracellular matrix molecules, in a wide range of diseases.

1.2 3D bioprinting

3D printing is a process used to create three-dimensional solid structures from a digital model, i.e. CAD (computer-aided design). The structure is then divided horizontally into several layers and each of these is printed sequentially by laying down the material until the entire desired solid has been constructed.

3D printing is a widely used process that allows the creation of complex structures using a lower quantity of material than other classic production methods.

Due to its great potential and its growth in the last years, 3D printing has been the subject of great growth and is now commonly used in many applications, including medicine, production, art and architecture. Among the different medical applications, cancer modelling, tissue engineering and regenerative medicine are particularly exploiting this technique, giving rise to the 3D bioprinting field.

3D bioprinting combines biomaterials, cells and, possibly, other biochemical factors to produce structures with the aim of imitating the characteristics of natural tissues and organs.

Although bioprinting approaches still need to be improved with regard to controlled cellular distribution, high resolution of the structure and placement in complex 3D fabrics, this innovative technique proved to be a crucial turning point in the biomedical field right from the outset.

Soft living cell-laden biomaterials used for creating structures in 3D bioprinting are called bioinks. A large range of biomaterials has been studied and produced for tissue engineering and regenerative medicine, aiming at maintaining great cell viability during short- and long-term culture, cell-cell and cell-ECM interactions and cellular diffusion.

An ideal bioink should have some characteristics including excellent bioprintability, high stability and mechanical integrity, non-toxicity, resistance to solubility when in contact with the cell culture medium, ability to promote cell adhesion. Other important factors for bioinks are convenience and ease of production, as well as maintenance of the designed shape.

For these reasons, it has been observed that a hydrogel is the best bioink for 3D bioprinting with cells encapsulation for the three-dimensional construction of tissues and organs.

1.2.1 Operating principles

3D bioprinting is a manufacturing process guided by digital information: the desired structure is modeled and generated using a Computer-Aided Design (CAD) file. The models are then translated into G-Code language, by means of a program, e.g. *Slic3r*, which is able to divide the structure into sections and generate step-by-step instructions for the printing machine.
According to their functional mechanisms and different bioink requirements, bioprinting processes can be classified under three major types, shown in Figure 1.2: inkjet-based bioprinting, extrusion-based bioprinting and laser-based bioprinting.

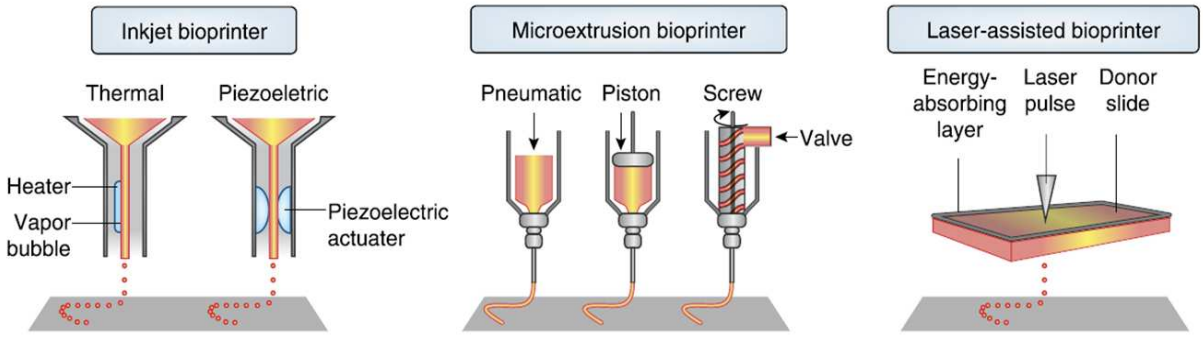

Figure 1.2 *Components of inkjet, extrusion and laser-based bioprinters* [10].

Inkjet bioprinting uses different energy sources such as thermal and piezoelectric to efficiently generate bioink droplets: thermal inkjet bioprinters use a heater so that the printhead is electrically heated to produce pulses of air pressure that force droplets out of the nozzle, while the second type uses pulses obtained from piezoelectric or ultrasonic pressure.
The optimal bioink to be used in this type of bioprinter should be characterized by a low viscosity in order to flow smoothly through the channel and the nozzle without causing clogging. Furthermore, immediately after the release of the bioink droplets the solidification process should occur. A suitable material would be a rheopectic liquid, which shows a time-dependent dilatant behavior (with a consequent increase in viscosity) when shear stress is applied, thus triggering the formation of droplets due to an increasing viscosity after leaving the nozzle.
The main advantages of thermal inkjet bioprinters are their low cost and high printing speed. However, the risk of exposing cells to mechanical and thermal stresses must be taken into account, and this factor is a significant drawback in the use of this category of bio-printers.
Extrusion bioprinting is a technique based on the use of mechanical or pneumatic forces, using pressurized air, a piston or a screw, to provide a continuous filament of bioink through a nozzle. The extruded material is directed to form the desired structure by moving the nozzle over the platform or by moving the latter under the nozzle; in any case, the 3D structures are formed through the continuous deposit of the material layer by layer. To successfully build 3D

structures in this way, the first layer must have structural integrity before the second is deposited. Consequently, parameters such as the rheology of the polymer and the mechanism of solidification are of crucial importance. The most suitable hydrogels for this bioprinting method possess shear thinning or thixotropic behaviors, so that shear forces help to decrease the viscosity and to align polymer chains in a preferential direction making them extrudable [(11)]. Thixotropy, a time-dependent shear thinning behavior, permits the hydrogel to be at rest in the channel, to get a low viscosity in the nozzle tip during extrusion and regain its stability after leaving the extruder [(12)]. The temporal control of gelation is essential to avoid premature gelation of the polymer solution while it is still in the bioprinter.

The main advantage of extrusion-based bioprinting technology is the fact that it is possible to print out high cell density hydrogels, a major goal for the bioprinting field because it can represent at best the physiological cell densities in tissues and organs.

Laser-based bioprinters use laser sources focused on an energy-absorbing substrate to generate pressures that force bioinks onto a substrate.

A laser-based device of this type is composed of a laser beam, a layer usually made of titanium or gold which has the function of absorbing laser energy and a layer of biological material such as the cell-laden hydrogel. This type of printer uses the generation of laser pulses focused on the absorbent layer to form a high-pressure bubble, which pushes the cell-laden hydrogel towards the substrate. The bioink suitable for this technology should be able to easily translate thermal energy into kinetic energy and show highly viscoelastic behavior.

The absence of nozzles is the main advantage in this type of bioprinter because the typical problem of nozzle clogging of the other bioprinting technologies already discussed doesn't occur in this case.

In this project an extrusion bioprinter was used, as it is the most promising in the field of biomedical applications and this is the best approach to manufacture heterogeneous models *in vitro* involving different types of cells or matrices; although it is characterized by a lower scanning speed compared to other technologies, with this it's possible to use hydrogel with higher viscosity and above all a greater cell density inside them.

1.3 Hydrogel

The search for suitable materials for the generation of biomimetic matrices that faithfully represent *in vitro* the complexity and three-dimensionality of ECM *in vivo* has led to the ever-increasing use of hydrogels [13]. The first application of hydrogels in the biomedical field is found in the 1960s with the introduction of photopolymerized hydrophilic matrices of pHEMA (poly-hydroxyethylmethacrylate) as material for contact lenses [14].
Now hydrogels exist in a variety of forms, and despite the use of different types of them in biomedical applications has experienced an exponential growth since then, it is still in continuous development today. In the biomedical field hydrogels have entered widely thanks to the interesting porous structure (very useful in these applications), to their biocompatibility and to the simplicity and rapidity of production.

1.3.1 Definition and properties

A hydrogel is a polymeric material with the ability to swell and retain a significant fraction of water within its structure, without dissolving in it. Recently, hydrogels have been defined as systems consisting of a three-dimensional network, thanks to the formation of chemical and physical bonds between macromolecules, and a liquid substance, usually biological a fluid or water, which fills the space between the macromolecules. In hydrogels, the liquid content of the polymeric matrix usually ranges from 20 up to 99% by weight. Also thanks to this large amount of liquid content, hydrogels are highly biocompatible. Biocompatibility is defined as the ability of the material to behave as a substrate allowing normal cellular activity, without causing any undesired effects or rejection reactions. Biocompatibility with regard to hydrogels depends on the characteristics of the used polymer, but also on the technique used for gelation, which could include cytotoxicity factors.
The ability of hydrogels to absorb water comes from hydrophilic functional groups attached to the polymeric backbone, while their resistance to dissolution results from crosslinking between chains.
From the mechanical point of view, hydrogels are characterized by an intermediate behavior between solids and viscous liquids. The liquid solution of the starting prepolymer, in which the bonds between the chains have not yet formed, shows a Newtonian behavior. After gelation, the 3D networks obtained assume viscoelastic behaviors or, in some materials, develop the characteristics of purely elastic materials [15].
An advantage in the use of hydrogels consists in the possibility of adjusting their properties. Degradation, the level of hydration of the matrix, and the mechanical properties, depend directly on characteristics such as the stiffness of the polymer chain, the polymerization density, the gelation technique and the swelling degree, which itself derive from the balance between hydrophilicity and hydrophobicity of the material. All these features can be modulated in order

to obtain materials with similar properties to those of human tissues, thus being able to use them in specific biological applications.

As regards the gelation technique, hydrogels are defined as *chemicals* when obtained through the formation of covalent bonds, or *reversible* or *physical gels* when secondary forces, such as ionic bonds or hydrogen bonds, are the main causes of formation of the three-dimensional network.

The latter are polymers that can be crosslinked without using any exogenous agent, thus minimizing the risk of chemical contamination or toxicity. In particular, ionic crosslinking exploits non-covalent interactions to bind polymeric chains; in this case a three-dimensional network of hydrogels is formed when molecules having opposite charges bind to each other (Figure 1.3).

Sometimes a small amount of crosslinking agent of opposite charge with respect to the starting polymer is also added.

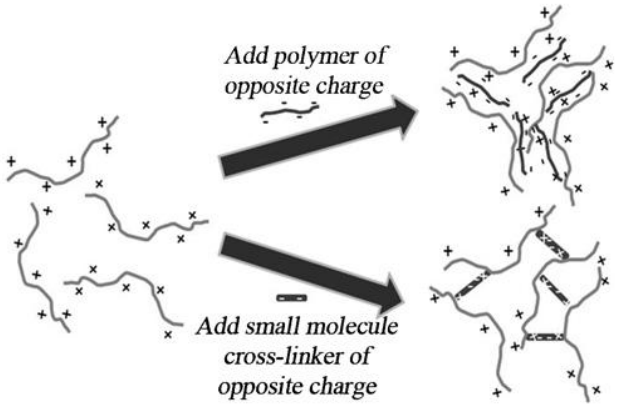

Figure 1.3 *Physical gelation driven by charge interactions* [16].

Another type of interaction that leads to a cross-linking of hydrogels is the formation of hydrogen bonds; these interactions are often characterized by a strong dependence on temperature, thus altering the rheology of the hydrogel with changes in temperature. In this case the hydrogel molecule, not having very strong bonds, can be disrupted by the simple application of shear stress (Figure 1.4) [12].

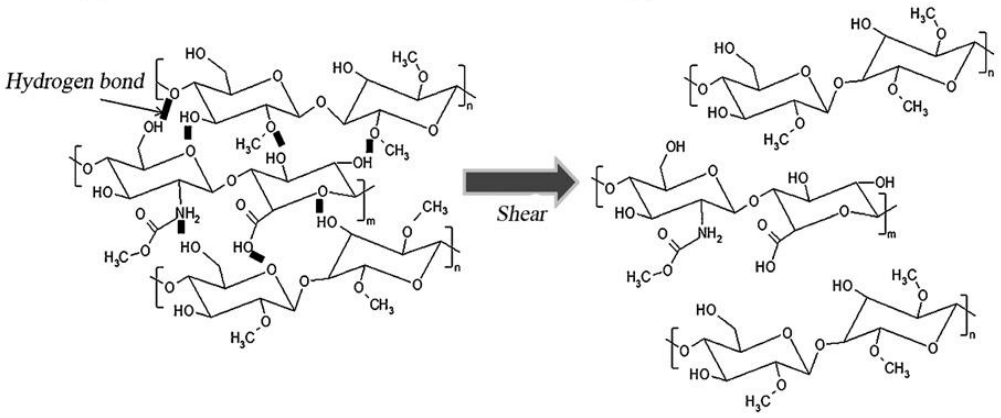

Figure 1.4 *Physical gelation driven by hydrogen bonding interactions, which can be disrupted by shear stress* [16].

A subclass of physically formed hydrogels is made up of hydrogels obtained from polymers called *smart* or *responsive*. The main characteristic of these polymers is given by the structure that can show great reversible changes in the physical-chemical behavior, as a response to small and usually rapid variations in the surrounding environment. An example that can occur in the hydrogels formed with this type of polymers is the passage from the collapsed state, in which the interactions between the polymer chains prevail, to the swollen one, where the greatest interactions occur between the chains and the solvent. This transition can take place in response to changes in temperature, pH, light or electric fields [17].

Unlike hydrogels formed by physical gelation, chemical hydrogels can be obtained by different polymerization methods, such as radical polymerization, high energy level irradiation, through chemical reactions between complementary groups, or by enzymatic polymerization.

Particularly interesting in the production of biocompatible hydrogels is photopolymerization, an example of radical polymerization and allows to convert a liquid prepolymer into a hydrogel in a rapid and controllable manner. The hydrogels obtained in this way can be polymerized using a UV or visible light source. These light sources interact with photoinitiators, i.e. light-sensitive compounds, to form free radicals in the prepolymer chains, which initiate the polymerization reaction to form the hydrogel.

The properties of light-curing hydrogels can therefore also be modeled through the control of other parameters such as photo-initiator concentration, polymer concentration and exposure to the light source.

On the other hand, in the photopolymerization process cells inside the hydrogel are in direct contact with potentially cytotoxic light sources and radicals, making it necessary to ensure accuracy in exposure time to the light source and a subsequent verification of cell viability, which may have been compromised. The choice of the ideal photoinitiator for cellular applications is therefore mainly made considering its cytotoxicity, trying to limit it as much as

possible. As regards the choice of the light source, this is instead constrained by the sensitivity interval of the photoinitiator used. In the biological field, wavelengths of 365 nm or 405 nm are usually used; at a lower wavelength of 258 nm, corresponding to the germicidal activity of UV light, the cells would be killed (Figure 1.5).

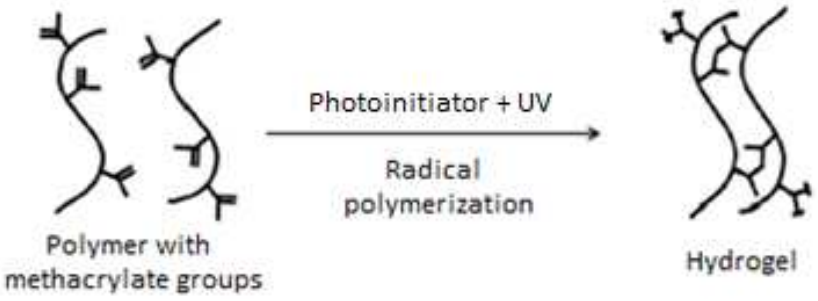

Figure 1.5 *Photopolymerization reaction of a polymer with methacrylate groups through UV radiation in presence of photoinitiator.*

1.3.2 Classification

A general classification of hydrogels can be made distinguishing them based on:

- **Gelation method**: physical or chemical crosslinking
- **Origin**: natural or synthetic

The first distinction according to the method of gelation has already been discussed in the previous paragraph.
Table 1.1 shows the most commonly used hydrogels as bioinks for 3D bioprinting in biomedical applications, distinguishing their natural or synthetic origin.

Table 1.1 *Most commonly used natural and synthetic hydrogels in biomedical applications.*

Natural hydrogels	Synthetic hydrogels
Agarose	Pluronic® F-127
Alginate	Polyethylene glycol
Chitosan	
Collagen type I	
Fibrin	
Gelatin	
Gelatin methacrylate	
Hyaluronic acid	
Matrigel™	

The natural-based hydrogels are obtained from natural proteins or polysaccharide-derived polymers, and are generally characterized by high biocompatibility, biodegradability and bioactivity in terms of cellular interaction. Natural-based hydrogels often have insufficient mechanical properties, relatively rapid degradation and variability in synthesis that makes their definitive characterization complicated. The biological origin can also lead in certain conditions to problems of transmission of pathologies and contaminations.
However, mechanical resistance and biodegradability can be modified starting from the base polymer, by the addition of functional groups to obtain crosslinking between the macromolecules and guarantee the formation of a more or less complex three-dimensional network.

- **Agarose** is a molecule of polysaccharides of natural derivation that undergoes a gradual and slow gelation at low temperatures. The gelation mechanism occurs in three phases: initiation, nucleation and pseudo-equilibrium. The solid-state agarose is rather brittle, but can maintain its shape for a long period of time even at different temperatures.
  Cell culture within agarose is not very favorable, because the rate of cell proliferation and the functions of cellular components are limited in this type of hydrogel [18]. Furthermore, to confirm this low efficiency in cell culture, low cell adhesion and diffusion were observed.
  In general, its high viscosity doesn't allow the use of this hydrogel in inkjet or extrusion bioprinting because it could frequently clog the nozzle. Agarose is therefore a material that can be used in laser-based bioprinting, thanks to its viscoelasticity and its rapid gelation mechanism.

- **Alginate** is a natural anionic polymer, typically obtained from brown algae, widely studied and used for many biomedical applications, thanks to its biocompatibility, low toxicity, low cost and rapid gelation using a calcium chloride solution ($CaCl_2$), thus exploiting the addition of Ca^{2+} divalent cations.
  Alginate hydrogels can be prepared by various crosslinking methods and their structural similarity to the extracellular matrices of living tissues allows extensive applications in wound healing, in the administration of bioactive agents such as small chemical drugs and proteins and in cell transplantation.
  Among its properties, alginate also gives viscosity to the hydrogel and is able to create the reticulations necessary for the structure to be self-supporting; the ionic crosslinking undergone by the hydrogel also makes it suitable for cellular encapsulation. Alginate extrusion-based bioprinting is one of the most popular techniques in the bioprinting community, while it is not very used in inkjet and laser-based bioprinting techniques.

- **Chitosan** is a linear polysaccharide molecule obtained from chitin deacetylation and is used in many applications in tissue engineering such as cartilage regeneration and

devices for antibacterial activity. Chitosan, which is generally used in extrusion bioprinting, is characterized by unstable mechanical properties and limited bioprintability, therefore it is an appropriate material for cellular encapsulation, but much less for the formation of large-scale scaffolding.

- **Collagen type I** is a triple helicoidal biocompatible protein obtained from natural sources; due to its structure, the collagen matrix facilitates both cell adhesion and cell attachment and growth. However, collagen type I shows limits because it remains in liquid state at low temperatures; this slow gelation rate makes bioprinting of 3D structures difficult, since the extruded collagen remains liquid for a very long time. Both extrusion and inkjet bioprinting can use collagen as bioink, however collagen must be deposited before crosslinking begins.

- **Fibrin** is a hydrogel that is produced by the enzymatic reaction between thrombin and fibrinogen, which are proteins that play a crucial role in blood coagulation.
  The rheology of fibrin hydrogel has long been studied because of its non-linear elasticity. The physical degradation of fibrin is quite rapid, which prevents a long-term culture; nevertheless, this hydrogel allows cell growth and proliferation. Due to the nature and characteristics of the two starting proteins, fibrin is usually not extruded; the extrusion bioprinting of the pre-crosslinked fibrin is almost impossible due to the strongly weak mechanical properties which don't allow the manipulation of the fibrin after gelation [12]. Fibrin is not even suitable for laser-based bioprinting, as it has a very delicate structure and could not withstand laser radiation. Furthermore, since it requires a prolonged crosslinking time and the properties are strongly dependent on the thrombin concentration, fibrin is hardly printable in a designed form.

- **Gelatin** is a natural protein obtained through thermal denaturation and partial hydrolysis of bovine or porcine collagen (typically), extracted from skin, bones and connective tissues. The extraction from collagen can be carried out by acid or basic means and depending on this it's possible to distinguish respectively between type A and type B products.
  The growing interest in its use derives from its high biocompatibility, biodegradability, easy handling and low cost. Unfortunately, gelatin in its natural state allows to obtain hydrogels usable only in certain conditions of temperature and concentration, and that are characterized by poor mechanical resistance. In order to increase the mechanical properties of the three-dimensional networks that constitute the natural hydrogel, and therefore to limit the instability of the gelatin at body temperature, it's possible to intervene on its macromolecules by adding molecules that allow to obtain crosslinking or alternatively through methacrylation of the amine groups, with varying degrees of functionalization.

Since gelatin properties are very favorable for cell culture, it caught a large interest for extrusion bioprinting: not only it is easily printable, but it also ensures ideal cell viability and final structure stability. Due to its properties and gelation mechanics, gelatin is not a good material choice for inkjet bioprinting. Instead, it has been successfully used in laser-based bioprinting as its viscoelasticity, thermosensitivity, structural stability and ability to maintain cells in precise positions without damaging them, are optimal characteristics in this bioprinting technique [19].

- **Gelatin methacrylate** (GelMA) is the denatured form of collagen with methacrylate groups conjugated to its side amine groups. It is widely used in tissue engineering thanks to its suitable biological properties and the possibility of adjusting its mechanical characteristics. Gelatin methacrylate doesn't allow high cell proliferation rates, but it's characterized by a fairly high mechanical strength, a low swelling ratio and it is easily mixed with other hydrogels in order to increase cell survival during culture; the crosslinking of methacrylate gelatin hydrogel, after an addition of a photoiniatior, takes place by exposure to a UV light source. GelMA hydrogel is widely used in extrusion bioprinting, because its viscosity is rather low at room temperature and it's therefore easy to extrude it, while its crosslinking rate can be adjusted by varying the exposure duration and the intensity of the UV light. Thanks to these properties it is possible to use gelatin methacrylate hydrogel also in inkjet bioprinting.
  GelMA has also been exploited for the laser-based bioprinting technique, in particular for the construction of scaffolds with a porous architecture [20].
  Since this synthetic hydrogel is one of the best for biomedical applications due to its biocompatibility and bioprintability, and since its use is optimal for extrusion bioprinting, GelMA has been chosen as the printing bioink for this project.

- **Hyaluronic acid**, which has a very similar behavior to collagen type I, can be found in almost all connective tissues and is the most important component of cartilage extracellular matrix.
  The greatest use of hyaluronic acid is in tissue engineering thanks to its high biocompatibility and ability to form flexible hydrogels. Chemical modifications to its functional groups are often made to improve its rheological properties, allowing it to be used as a bioink; nevertheless, hyaluronic acid has a quite slow gelation rate and poor mechanical properties.
  Hyaluronic acid, although used also alone in extrusion bioprinting, is often mixed with other hydrogels to improve its bioprintability and tendency to solidify.
  The use of hyaluronic acid hydrogel in inkjet bioprinting is not optimal because it's a very viscous material and has a slow gelation rate; instead, it has been used in laser-

based bioprinting, combining it with other hydrogels such as fibrin [21] to facilitate crosslinking and make it faster.

- **Matrigel™** is a commercial product and is a gelatinous ECM protein mixture; this hydrogel manages to promote cell growth from tissue fragments. Matrigel™ is highly expensive and thermally reversible material, but it also ensures a higher degree of cell viability compared to most of the other hydrogels once 3D bioprinted.
  As per extrusion bioprinting, it's essential to print Matrigel™ before the complete crosslinking. It has not yet been possible to use Matrigel™ as a bioink in inkjet bioprinting but so far it has only been used as a substrate to place and pattern cells [22]. Instead, its viscosity and ability to thermally crosslink, make it a suitable bioink for laser-based bioprinting.

The synthetic hydrogels are obtained from polymers by nature hydrophobic and are chemically more resistant, compared to natural polymers, through flexible and reproducible production processes. It has been shown that synthetic hydrogels allow for the encapsulation of cells that remain viable and metabolically active over time. However, lacking bioactive structures able to guarantee the response of the tissues in which they are injected, synthetic hydrogels don't promote and integrate with biological processes and for this reason they need functionalization. Their mechanical resistance is generally high and implies low degradation rate and therefore greater durability. Mechanical properties and degradability are easily controlled and can be suitably balanced through initial hydrogel design, by varying some factors during their synthesis.

- **Pluronic® F-127** is a trade name for a synthetic poloxamer-based polymeric compound, that crosslinks as the temperature increases, so for this material a reverse gelation takes place. Pluronic® when used as a bioink can undergo curing by exposure to UV light; the chemical crosslinking process helps the hydrogel to be more resistant to thermal degradation. Pluronic® hydrogel can be used as a bioink in extrusion bioprinting only above 20 °C, because at lower temperatures its bioprintability is not acceptable. However, since it is characterized by a high viscosity and is very thermosensitive, it's problematic to use it with inkjet bioprinting, which is therefore avoided; laser-based instead is not a bioprinting technique suitable for this hydrogel because it is not viscoelastic.
- **Polyethylene glycol** (PEG) is a linear polyether hydrophilic compound which can be conjugated to proteins, enzymes and other biomolecules.
  PEG is a water-soluble material and has the advantage that, through the variation of some parameters during its synthesis, it is possible to modify its mechanical properties. Nevertheless, the main limitation of polyethylene glycol is its poor mechanical strength;

this problem can be overcome by adding diacrylate and methacrylate groups. Therefore, the hydrogels of diacrylate polyethylene glycol (PEG-DA) and methacrylate polyethylene glycol (PEG-MA) are easily used as bioinks in all bioprinting techniques.

1.3.3 Biomedical applications

Thanks to their properties of biocompatibility, biodegradability and microporosity, hydrogels have found an increasing use over the years. Among the various applications, the main ones consist on systems for drug release, biosensors and use as biomimetic materials, thanks to their ability to recreate a 3D matrix for the encapsulation of cells.

Tissue regeneration is achieved by the development of stem cells. Stem cells are undifferentiated cells, therefore for which the function within the organism is still undefined; these remain so until a stimulus intervenes that causes them to differentiate into specialized cells to fulfill a specific function. Throughout human or animal life, stem cells within tissues act as an internal repair system, with the ability to replace other damaged or dead cells.

The goal of tissue engineering is to create scaffolds, namely three-dimensional structures, able to simulate the extracellular environment and that provides cells the support for growth, proliferation and differentiation, temporarily replacing the mechanical functions of the natural extracellular matrix and gradually degrading to leave space for the matrix synthesized by the cellular component.

The main role of these scaffolds is to provide cells with appropriate stimuli, thanks to biocompatible matrices with specific mechanical properties, so as to obtain the formation of new tissues. In particular photopolymerizable and degradable biomaterials are widely used in the field of tissue engineering for bone, cartilage and hepatic tissues.

Hydrogels can therefore be exploited as structures for the *in vitro* study of cellular behavior in different conditions, such as pathologies, thanks to their efficiency in enclosing cells within an environment similar to the physiological one, which allows simulating in a more realistic way the interactions that occur among the different cells and between cells and ECM.

The extracellular matrix is formed by molecules secreted by the cells and with which they interact. Support for the structure and mechanical solidity are provided by a group of fibrous proteins such as fibronectin, collagen and laminin, while proteoglycans fill the voids present in the ECM and having a strongly negative charge they allow the absorption of water and biological fluids, keeping the environment hydrated (Figure 1.6) [(4)].

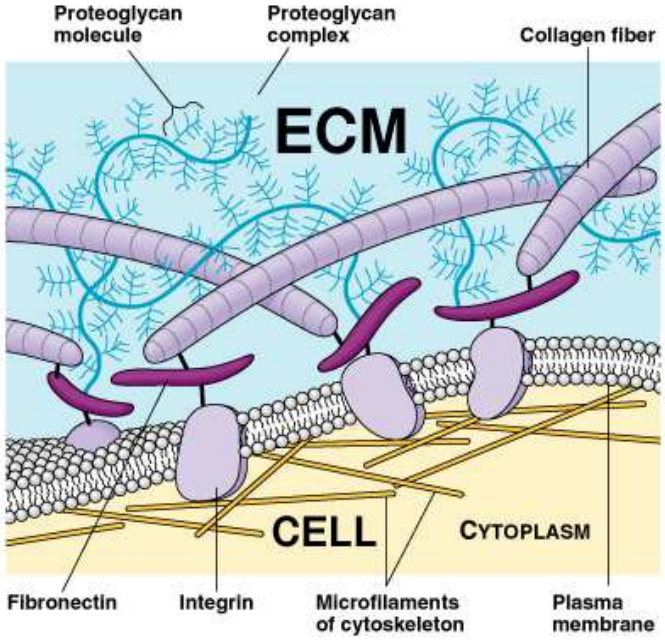

Figure 1.6 *Schematic representation of the structure of the ECM and the interactions between the cell and the components of the extracellular environment.*

In addition to acting as a mechanical support for cells, ECM also represents a bioactive and dynamic environment that regulates all cellular functions [(23)].

Hydrogels represent very promising materials to produce biomimetic matrices as they show many structural similarities with the ECM components: the three-dimensional and viscoelastic structure of the hydrogels is very similar both in its structure and in its function to the ECM protein group. The ability to retain high volumes of water then provides a level of hydration to the hydrogel matrices similar to that found *in vivo*.

Furthermore, the presence in their structure of a network of interconnected micropores favors the transport of oxygen and nutrients, which is a key characteristic of the natural extracellular environment.

1.4 Neuroblastoma

Neuroblastoma, an immature tumor of the nervous system, is the most common extracranial tumor in childhood. It represents over 7% of malignant tumors in patients under the age of 15 and about 15% of all deaths from pediatric oncology.
It is a tumor that originates from neuroblasts, cells present in the sympathetic nervous system, a part of the autonomous nervous system that controls some involuntary functions such as breathing, digestion or heartbeat. In particular, neuroblasts are immature or developing cells that are found in the nerves and are spread throughout the body: adrenal glands, neck, thorax or spinal column. For this reason neuroblastoma can arise in different locations; in most cases it occurs at the level of the adrenal glands, which are located above the kidneys or in the nerve ganglia (agglomerates of nerve cells) in the abdomen, while almost all the remaining cases involve the ganglia along the vertebral column at the level of neck or chest or pelvic.

1.4.1 Mechanism of invasion and metastasis

The term *metastasis* indicates the spread of a cancer in a different body part from where it started. Metastasis develops most commonly when some cancer cells detach from the main tumor, then entering the bloodstream or lymphatic system, which carry fluids throughout the body. This detachment and transport mean that cancer cells can move away from the original tumor, forming new tumors when they settle and grow in a different part of the body.
It has been studied that neuroblastoma is a metastatic tumor in 70% of patients at the time of diagnosis. The ability of neuroblastoma cells to affect distant organs such as bone marrow and bone is the result of interactions between selected tumor cells and the surrounding microenvironment of a specific organ [(24)].
The mechanisms that promote neuroblastoma cells metastasis, which is the leading cause of death in this cancer, are still poorly known, compared to the knowledge of the heterogeneous nature of the primary neuroblastoma.

1.4.2 Exosomes in neuroblastoma

Exosomes are extracellular vesicles of nanometric dimensions (50-100 nm) derived from the multivescicular bodies of the endocytic pathway and released from normal and neoplastic cells. Tumor-derived exosomes have been shown to be able to transport molecules that promote cancer growth and dissemination. In particular, those from neuroblastoma express a discrete set of molecules involved in defense response, cell differentiation, cell proliferation and regulation of other important biological processes; therefore, these vesicles can play an important role in modulating the tumor microenvironment and representing potential tumor biomarkers [(25)].

1.5 Aim of the thesis

The present thesis work is aimed at the investigation of the potential of a biocompatible and light-curing gelatin methacrylate-based hydrogel in 3D bioprinting in order to evaluate the viability and migration of neuroblastoma cells.

To carry out this research, some main steps have been followed: firstly, the optimization of the preparation of gelatin methacrylate, trying to improve the accuracy in the synthesis so as to obtain the desired polymer.

Subsequently by using gelatin methacrylate, the hydrogel was produced at different concentrations, in order to obtain a suitable support material that allows cells to find an adequate environment capable of promoting their adhesion and proliferation.

Once the optimal hydrogel concentrations allowing a good bioprintability and stiffness of the structure were identified, it was necessary to design and generate printing structures that would allow an evaluation at least qualitative of cell migration.

Mechanical tests were then performed to evaluate the properties of the hydrogels, in particular micro-rheological studies on the samples in dynamic conditions in order to obtain parameters related to the hydrogel viscoelastic properties and relate them to printability.

An analysis was carried out both on the polymer and on the hydrogel to estimate their melting temperatures. The hydrogel at different concentrations was then subjected to a test in order to evaluate its swelling, a very important factor especially in cell culture applications.

The biological validation was then considered through the 3D bioprinting of the optimal hydrogels with encapsulated cells inside, or cells and exosomes together according to the experiment carried out. Following these tests, the structures obtained were kept under control for different periods of time in order to evaluate the resistance of the structure and above all the behavior of cells within them, in terms of viability, proliferation and migration.

Chapter 2

Materials and methods

This chapter describes the procedures and protocols followed during the activity, starting from the synthesis of the polymer, followed by the preparation and optimization of the gelatin methacrylate hydrogel. Subsequently, in order to obtain a characterization of the materials used, the mechanical tests carried out on the hydrogel and polymer are explained.
The choice of the structures used for the 3D bioprinting will then be analyzed and what concerns the performed cellular tests is introduced.

2.1 3D bioprinting

The specifications of the available 3D bioprinter to carry out the tests will be briefly illustrated, followed by the reasons for the adopted printing geometries and the ideal conditions of the used hydrogel to be suitable for 3D bioprinting.

2.1.1 3D bioprinter

The 3D bioprinter used in this study is the INKREDIBLE model of Cellink® company, shown in Figure 2.1.

Figure 2.1 *3D bioprinter INKREDIBLE of Cellink® company.*

It is an extrusion-based bioprinter equipped of a compressor conveying air to the two extruders. It is therefore possible to make 3D prints using both extruders, which can contain different hydrogels and operate at different extrusion pressure values. The printing pressure can be adjusted for values that have a maximum of 400 kPa if only one extruder is in action, while by printing two hydrogels together it's possible to reach a maximum of 200 kPa per extruder.
It is also crucial to choose the ideal nozzle, since its size directly influences key parameters determining printing precision and the necessary pressure. Commonly used sizes range from 0.25 mm to 0.41 mm in diameter. It must be taken into account that nozzles of small diameters guarantee greater precision but require higher pressures which, in the presence of encapsulated cells in the hydrogel, can cause their death during the bioprinting process.
A disadvantage of this type of bioprinting is the fact that the dimensions of the extruded filament are not constant, so that it becomes necessary to adjust the pressure also during printing; one of the consequences could be the non-adhesion of the filament to the structure already deposited, thus causing the failure of the printing.
This model of bioprinter is also equipped with a UV-A source with a 365 nm wavelength which allows the filament to be reticulated during the printing process, if the material is photosensitive.

2.1.2 Structure design and G-Code generation

The design of the structures printed in the experiments was carried out in *AutoCAD*, so after their creation they were exported as STL file (STereo Lithography interface format or Standard Triangle Language acronym) and imported on *Slic3r*, a program used to generate the G-Code files containing all indications in machine language so that they are recognized by the bioprinter.
Among the various settings, *Slic3r* allows to set the height of each layer that will compose the final structure, the size of the nozzle used, the printing speed of the extruders expressed in mm/s, and, since the printer operates by first depositing the hydrogel that form the perimeter of the desired shape, it's possible to set the percentage and pattern of infilling the structure.
For the first part of the research, i.e. the optimization of the compositions of the hydrogel to evaluate to which concentration of gelatin methacrylate corresponds a better structure in terms of bioprintability and stiffness, the structure shown in Figure 2.2(a) was used, formed by a central chamber and two side chambers; only one extruder is used for printing this structure.
The central chamber is bound by a wall whose internal perimeter is a 1.88 mm side dodecagon, while a 4.55 mm side dodecagon, concentric with respect to the central chamber structure, constitutes the outer perimeter.
Dodecagons have been chosen over circles since the printer is not able to execute the printing of circular figures in the best way, so the goal was to approximate circles with polygonal figures.
The distance between the internal and the external dodecagon is 4 mm; the walls of the structure are 1 mm wide, except for the two separators, which vary in thickness between 1 and 1.5 mm

and have the function of dividing the external structure into two different chambers. Figure 2.2(b) shows how the described structure appears in *Slic3r*.

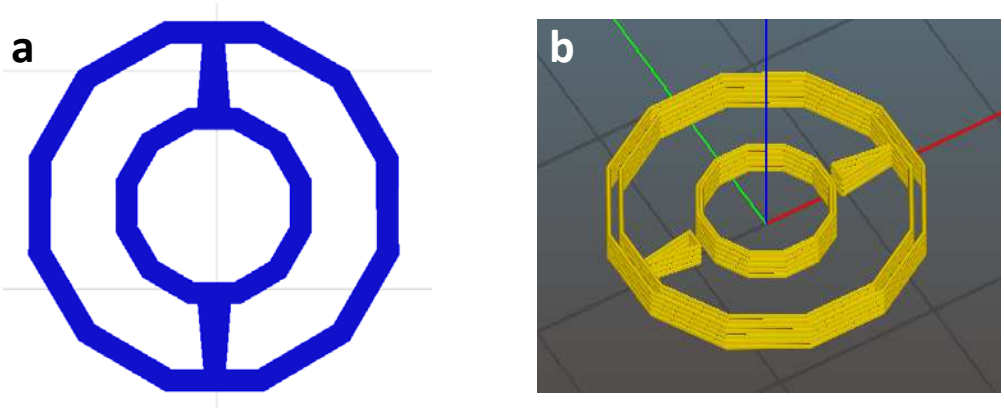

Figure 2.2 *Two dodecagons printing structure shown in a) AutoCAD and b) Slic3r.*

Once the best performing hydrogel concentrations were identified, different models were studied and tested to face the second step of the research, that is a preliminary evaluation of cell migration within them.
The main criteria that a good printable structure model must satisfy are basically three:

- the structure must be simple to implement and not too detailed;
- a contact surface must be present between the cell-laden hydrogel and the one without cells in order to make cell migration possible;
- being able to effectively monitor the interfacial area to analyze the phenomenon of migration over time.

Among the various configurations proposed that respected these criteria, the most useful for the purposes of this study were the following structures, both with similar "ladder-like" shapes and printed using both extruders.
The first structure (Figure 2.3) is formed by two parallelepipeds, of equal length and height but with different width, connected to each other through eight equidistant channels.
The two parallelepipeds have a length of 23 mm, are 0.6 mm high, and have different widths: one is 2 mm while the second is 1 mm wide. The connector channels are 10 mm long and 0.5 mm wide, and they have the same height of the two parallelepipeds.
The parallelepiped with the greater thickness will represent the cell-laden hydrogel, while the other one and the channels will be printed using the hydrogel without cells inside.
A structure with this form was used in order to investigate the cell migration in the contact line between the two hydrogels, namely at the interface between the channels and the widest parallelepiped. The part of the structure containing the cells was designed with a greater

thickness than the other one in order to facilitate alignment and orientation of the structure with the naked eye, an impossible task to perform if the two sides were identical in size since cells are only identifiable under the microscope.

To carry out an accurate research on migration it's necessary to monitor the area in which it occurs over a defined period of time, so the idea of using the channels to create contact between the two hydrogels has the purpose of uniquely identifying the interfacial area of separation, making it much easier to follow the phenomenon over time. If, for example, the two parallelepipeds were designed side by side; in the absence of the channels, it would have been impossible to recognize the same area at the interface at different times for a correct evaluation of cell migration.

The 0.6 mm height of the structure is justified by the fact that the printing will be performed using a nozzle of 0.28 mm in diameter, so the design involves a printed structure consisting of two bioink layers. A single layer structure would not have the structural solidity necessary to withstand the conditions of cell culture for several days after printing and it would break.

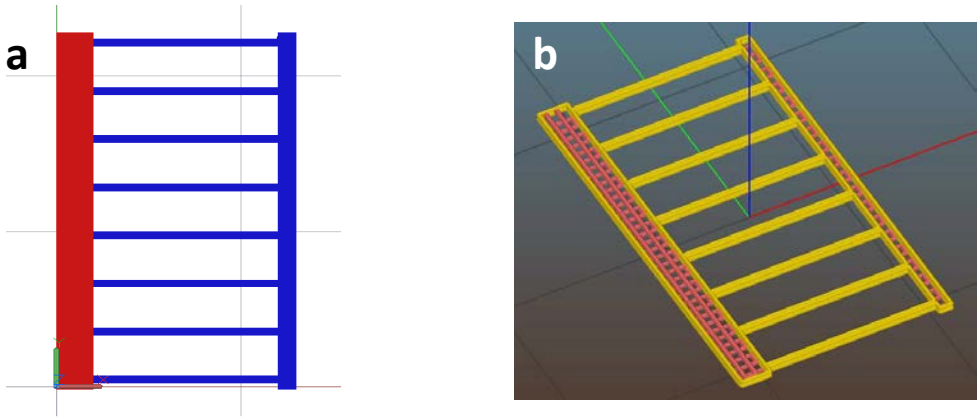

Figure 2.3 *Two parallelepipeds connected by eight channels printing structure shown in a) AutoCAD and b) Slic3r; the latter represents a printing preview, the lines show how the hydrogel will be distributed during printing and represents the filling pattern of the structure, set with a percentage of 40%.*

The second structure (Figure 2.4) also has the shape of a ladder, with the same dimensions as the previous case as regards the length of the channels, the width of the two parallelepipeds and the height of the entire structure. The number of channels is however reduced to six, and are designed with a double width compared to the previous case, therefore measuring 1 mm. The length of the entire ladder is also modified, and is here shortened to 22 mm.

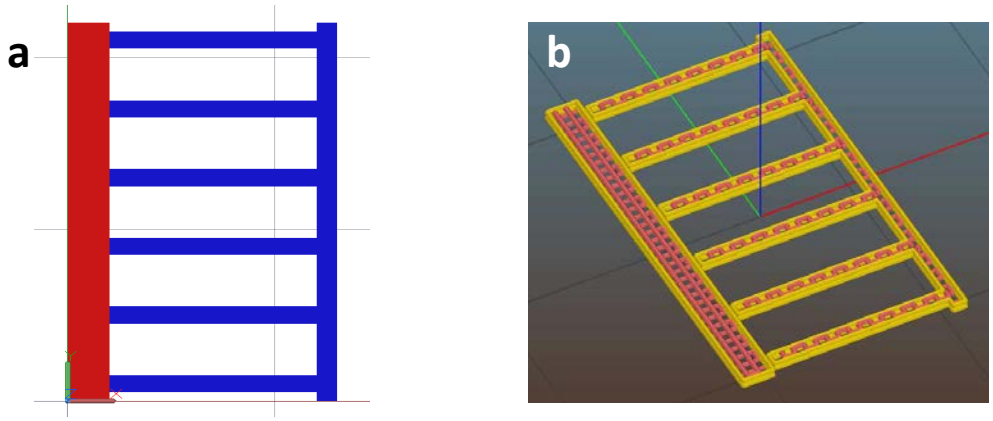

Figure 2.4 *Two parallelepipeds connected by six channels printing structure shown in a) AutoCAD and b) Slic3r.*

The choice to enlarge the connection channels up to 1 mm was aimed at obtaining an even more stable and resistant structure, with the goal of making the printed object last for a longer time in culture.

A problem that arose following the printing of the six-channel structure is the fact that observing it under a microscope with a 10X magnification (the most suitable one for a migration analysis due to the cell size that can vary between 10 and 100 micron) it is not possible to visualize the entire channel thickness in one image, since it exceeds the maximum observation field dimensions. This limitation is removed with the use of the eight-channel structure which, being thinner, allows this observation.

A preliminary study was also carried out on structures with similar shapes as the latter but with reduced width and length, in order to make them amenable to printings in standard multiwell plates. This approach will need further characterization and will be the object of future studies.

2.1.2.1 List and name of the printing structures

- **Three chambers**

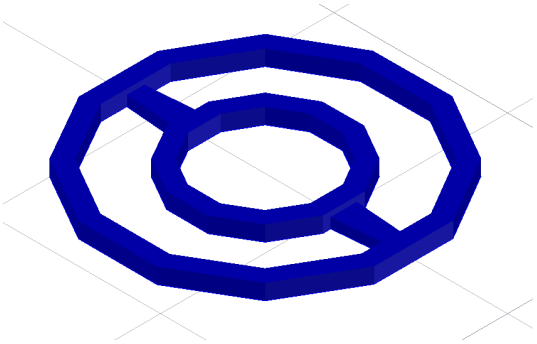

- **8 channels ladder**

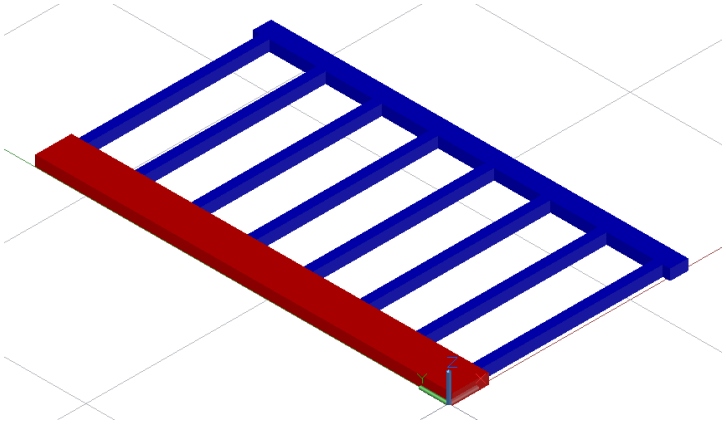

- **6 channels ladder**

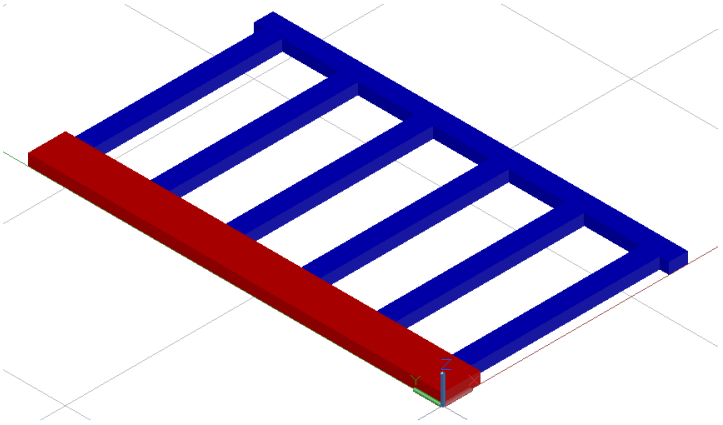

2.1.3 Hydrogel conditions

Each hydrogel used for 3D bioprinting has different properties and thus requires various pretreatments in order to obtain a good printability, in addition to the accurate setting of the different printing conditions.

The gelatin methacrylate-based hydrogel, which is the bioink used in this research, is characterized by a strong thermoreversibility, so it can be reused by heating it once it has thickened. The strong sensitivity of GelMA hydrogel to temperature results in significant changes in properties such as viscosity and a rapid transition from a liquid to a gel state and vice versa (the so-called sol-gel transition or gelation) even following small magnitude ΔTs.

Obviously, the ideal state of the hydrogel at the time of printing must be not too liquid since there would be a collapse of the three-dimensional structure whose shape would no longer be defined as the desired design, nor in a pure gel state because in addition to the need for providing more pressure to allow it to be extruded from the nozzle, it could form a grainy structure which is also not ideal and well defined, or could even clog the nozzle.

At temperatures lower than about 30 °C, thermoreversible sol-gel transition of GelMA occurs, which leads to partial gelation. Reducing the temperature below about 30 °C causes an increase in viscosity but can complicate printing due to the frequent clogging of the printing nozzle [(26)].

GelMA hydrogel must first be brought to the liquid state, by means of a bath at a temperature of 37 °C, loaded with cells, and moved into the extruder syringe used in the 3D bioprinter. It must then be cooled inside a refrigerator set at a temperature of 4 °C.

The cooling time necessary to obtain the proper consistency of the hydrogel varies according to factors such as: *i*. the concentration of the hydrogel, *ii*. its quantity contained in the extruder, *iii*. the time needed to calibrate the printer, *iv*. the printing time to obtain the structure, *v*. the number of desired successive printings and also *vi*. the laboratory temperature at the time of the experiment.

The typical refrigeration time employed for the applications in this research study was between 8 and 15 minutes, depending on the needs of the specific experiment, in particular a shorter time if the concentration of the hydrogel used was greater and on the contrary a longer cooling when the hydrogel had a lower polymer concentration.

2.2 Synthesis of gelatin methacrylate

Gelatin is a natural biopolymer derived from collagen denaturation; it is an excellent material for obtaining hydrogels, thanks to its gelation properties.

We thus chose to synthesize and characterize a gelatin-based hydrogel modified with methacrylic groups, which allow the polymeric chains of the obtained material to crosslink after exposure to ultraviolet radiation in the presence of a photoinitiator agent.

The gelatin used in this research study is derived from porcine skin, obtained by means of an acid treatment, and is named type A gelatin; it is marketed by Sigma Aldrich® company (Sigma Aldrich, G1890) and has a gel strength of about 300 g Bloom.

Gelatin methacrylate was obtained through a methacrylation reaction between the hydroxyl groups and primary amino groups of the biopolymer chains, the lysines, and the methacrylic anhydride (MAA), also provided by Sigma Aldrich®, under suitable conditions of pH, temperature, and initial concentration of reagents. The schematic representation of the reaction is shown in Figure 2.5.

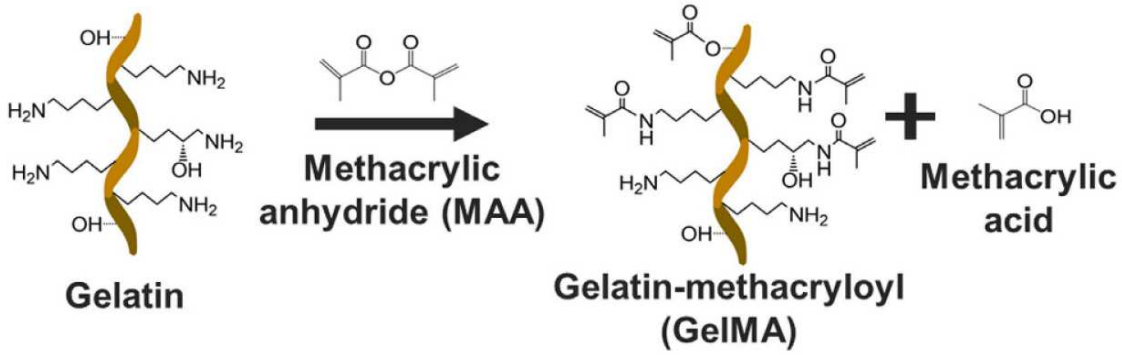

Figure 2.5 *Schematic representation of the synthesis reaction of GelMA, where NH_2 are the primary amino groups and OH are the hydroxyl groups* [27].

Several methods exist for the production of gelatin methacrylate, starting with its original synthesis developed by Van Den Bulcke *et al.* (2000) [28].

This method requires that, after dissolution of gelatin in 7.8 pH 100 mM phosphate buffer (PBS, Phosphate buffered saline) at 50 °C and under vigorous stirring at 700 rpm, methacrylic anhydride is slowly added dropwise in quantities varying between 0.8 and 2 mL per gram of gelatin depending on the degree of substitution required. The reaction lasts about two hours, during which pH measurements are performed (using a pH meter or a litmus paper) until it stabilizes at the desired value of 7.8. The addition of methacrylic anhydride tends to lower the pH of the solution, since it's an acid; this lowering must be counterbalanced to maintain the desired pH by adding drops of sodium hydroxide solution (NaOH), which is basic. A 3 M, 5 M or 10 M solution of NaOH can be used, for example, and clearly according to this difference

the quantity of drops of basic solution required for pH equilibrium will be different. If the addition of NaOH brings the solution to a pH higher than 7.8, this can be lowered by adding a few drops of sulfuric acid (H_2SO_4).
Following the two-hour reaction carried out at stable pH, the obtained mixture is diluted 1:10 in 7.8 pH 100 mM PBS and dialyzed with 14 kDa MWCO (molecular weight cut-off) membranes for 48 hours against distilled water under stirring at 500 rpm, in order to remove methacrylic acid produced and any traces of unreacted methacrylic anhydride and thus obtain pure GelMA.
The reaction product is then lyophilized, resulting in a white solid.

The following is the protocol for the preparation of a liter of 7.8 pH 100 mM PBS:

- 1 L of ultrapure water (Milli-Q H_2O);
- 25.41 g of sodium phosphate dibasic heptahydrate ($Na_2HPO_4 \cdot 7H_2O$);
- 0.63 g of potassium dihydrogen phosphate (KH_2PO_4);
- solution stirred at 800 rpm until the two solutes are completely dissolved;

where ultrapure water means a water that has been purified and deionized to a high level by a purification system made by Millipore Corporation®.

The detailed protocol for the synthesis method used in the research is the following:

- water bath heated to 50 °C and stirred;
- 10 mL of 7.8 pH 100 mM PBS placed in the water bath and heated to 50 °C;
- 1 g of gelatin from porcine skin (type A) dissolved in 7.8 pH 100 mM PBS stirred at 400 rpm for 20 min;
- 0.14 mL of MAA (methacrylic anhydride) per gram of gelatin added in drops;
- 2 h of reaction at 7.8 pH under stirring at 700 rpm and 50 °C;
- pH checked every 15-20 min and eventual adjustment with drops of 3M NaOH if pH<7.8 or H_2SO_4 if pH>7.8; less frequent pH adjustments as the reaction continues since pH stabilizes;
- solution centrifuged for 4 min at 4000 rpm;
- solution diluted to 1:10 in 7.8 pH 100 mM PBS;
- reaction mixture dialyzed with a 14 kDa MWCO (molecular weight cut-off) membrane in deionized water under stirring without heating for 48 h, changing deionized water every 3 h;
- solution frozen and freeze-dried leading to a white solid.

Another method of synthesis of gelatin methacrylate polymer applied in this research has been developed by Brigo *et al.* (2017) [29]. This method is based on the same principles as that of Van Den Bulcke *et al.* (2000) and up to the passage of the reaction is analogous to it.
The main difference lies in the recovery and purification phase of GelMA, which no longer occurs by dialysis with membrane and lyophilisation, but by precipitation in large excess of ethanol at a temperature of -20 °C, and rinsed twice in ethanol. In this way, GelMA pellets are obtained which are then vacuum-dried for at least 24 hours.

The detailed protocol for this second synthesis method is the following:

- water bath heated to 50 °C and stirred;
- 10 mL of 7.8 pH 100 mM PBS placed in the water bath and heated to 50 °C;
- 1 g of gelatin from porcine skin (type A) dissolved in 7.8 pH 100 mM PBS stirred at 400 rpm for 20 min;
- 0.14 mL of MAA (methacrylic anhydride) per gram of gelatin added in drops;
- 2 h of reaction at 7.8 pH under stirring at 700 rpm and 50 °C;
- pH checked every 15-20 min and eventual adjustment with drops of 3M NaOH if pH<7.8 or H_2SO_4 if pH>7.8; less frequent pH adjustments as the reaction continues since pH stabilizes;
- GelMA precipitated in large excess of ethanol at -20 °C (GelMA:ethanol volume ratio equal to 1:8);
- solution centrifuged for 10 min at 3000 rpm and 4 °C;
- ethanol removal and second precipitation in large excess of ethanol at -20 °C;
- solution centrifuged for 5 min at 3000 rpm and 4 °C;
- GelMA pellets dried under vacuum for at least 24 h.

The operating conditions of the reaction are very strict, especially regarding temperature and pH.
The reaction temperature must be precisely kept at 50 °C and it is not possible to increase it to improve the reaction kinetics because above this temperature value the methacrylic anhydride would start to hydrolyze before it even reacts.
This reason also partly influences the need for a precise pH value, which must be at a value of around 8, better if 7.8; in fact, if there was a more acidic reagent solution, the reaction would not start because the hydroxyl groups and the primary lysins would not undergo the hydrolysis necessary to bind to the methacrylic groups. On the contrary, if the detected pH was greater than the desired value, it would not be a problem for the OH groups and the primary amino groups, but instead the methacrylic anhydride would hydrolyze, thus not completing the reaction.

2.2.1 Purification

The main difference between the various methods of synthesis of gelatin methacrylate applied in this study lies in the stage in which the purification of the solution obtained from the reaction takes place, which allows to obtain the final product.

Most of the articles found in literature use the classic method with separation of methacrylic anhydride and methacrylic acid from the solution through the use of membranes and subsequent freeze-drying. Since the laboratory in which this research activity was carried out is not equipped with a lyophilizer, it was necessary to use the equipment of external sites. Furthermore, following freeze-drying, the product obtained was never suitable for the applications of interest, because when this GelMA was used to produce the hydrogel, it quickly denatured and could not be used for bioprinting applications. This failure could derive from possible operative errors in one or more passages of the synthesis, and since the main difference of this method lies in the purification step, the error could be identified in the separation with membranes; therefore a future development in order to improve the accuracy of this synthesis is the optimization of this separation step.

For these reasons, the method of production of gelatin methacrylate proposed by Brigo *et al.* was mainly employed, which provides for the precipitation of the reaction product in ethanol, which has the function of extracting the undesired by-products and any unreacted reagent from the synthesized GelMA.

Ethanol has the function of purifying GelMA but it's then necessary to remove the ethanol absorbed from the product pellet by vacuum drying, to avoid problems in subsequent steps such as bioprinting with cells seeded inside GelMA hydrogel; the drying process takes a long time, at least 24 hours.

An attempt was made to vacuum-dry with the aid of a temperature increase up to about 50 °C in order to reduce the drying time and to improve its efficiency, but no gain was observed especially in terms of efficiency, so this option was discarded in following synthesis reactions.

A first precipitation in methanol was also tested to improve the efficiency in separation step, with subsequent rinsing in ethanol; the result was good, but since it did not bring any significant improvement to the use of ethanol alone it was preferred to avoid its use due to its toxicity.

2.3 Hydrogel preparation

Hydrogels are polymeric networks with hydrophilic properties; synthetic polymers are usually hydrophobic and chemically stronger than natural polymers [30].

In general, the fundamental components in the preparation of the hydrogel are monomer, initiator and solvent, which can be water or a biological fluid.

For cellular applications the choice of the ideal photoinitiator must be made mainly taking into consideration its characteristics of cytotoxicity and solubility in the used solvent. Several studies such as Williams *et al.* (2004) showed a comparison between the main photoinitiators on the market, demonstrating how 2-hydroxy-4′-(2-hydroxyethoxy)-2-methylpropiophenone (Irgacure 2959) (Figure 2.6) is among those the one with less cytotoxicity [31]; therefore, this is the photoinitiator chosen for the preparation of the hydrogel in this study.

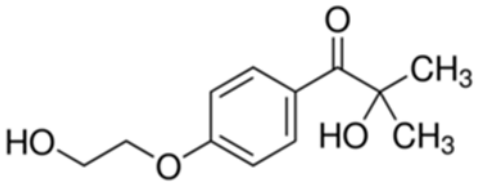

Figure 2.6 *Chemical structure of the photoinitiator 2-hydroxy-4'-(2-hydroxyethoxy)-2-methylpropiophenone.*

As regards the fluid used as a solvent for the preparation of the hydrogel, PBS 1X is usually used in the biological field, which is simply a dilution of PBS 10X with ultrapure water (Milli-Q H2O).

The steps in preparing the hydrogel involve the weighing of GelMA pellets, their dissolution in a certain amount of PBS 1X depending on the desired hydrogel concentration and the addition of the photoinitiator. The latter was initially tested at 0.5% w/v concentration in PBS 1X, but the obtained hydrogel was not sufficiently crosslinked after UV exposure; the concentration of photoinitiator was then doubled, since in literature it is found that its maximum concentration used is 1% w/v, due to its cytotoxicity [32].

Photoinitiator Irgacure 2959, if triggered by UV radiation, releases radicals (Figure 2.7) that cause radical crosslinking.

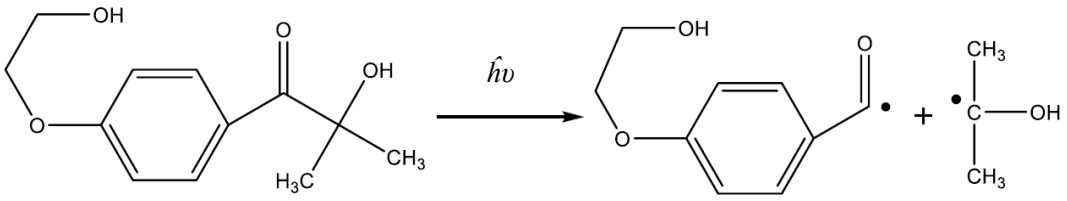

Figure 2.7 *Mechanism of radical dissociation from Irgacure 2959 following the $\hat{h}\upsilon$ energy absorption [33].*

The protocol used for the hydrogel production is the following:

- water bath heated to 50 °C;
- PBS 1X placed in the water bath and heated to 50 °C;
- 1% w/v photoinitiator weighed and dissolved in PBS 1X at 50 °C and under stirring at 600 rpm;
- gelatin methacrylate pellets added to PBS at 50 °C and 600 rpm;
- once the pellets are dissolved, 15 min of stirring at 1000 rpm and 50 °C;
- solution centrifuged for 3 min at 1000 rpm;
- solution placed in a water bath at 37 °C a few minutes to keep liquid the hydrogel.

2.4 Material characterization

During this activity micro-rheological studies were carried out on the samples in order to obtain parameters related to the hydrogel viscoelastic properties and to relate them to printability.

2.4.1 Dynamic mechanical analysis

One of the tests carried out is dynamic mechanical analysis (DMA), which is a type of mechanical test used to evaluate the viscoelastic behavior of a material, in this case the hydrogel, with the aim of determining its response when subjected to a dynamic stress, with sinusoidal trend and increasing frequency. The response of the material to the stress is thus detected, and the phase lag between stress and strain is measured; this is called damping factor and indicated with the symbol δ.
Through DMA analysis it is possible to derive the behavior of the polymers as a function of temperature, thus determining the viscosity curve and the glass transition temperature.
Two other important data for the polymers mechanical characterization obtained from this type of analysis when a shear stress is applied, are the storage modulus G^I and the loss modulus G^{II}, or E^I and E^{II} in the case of axial stress:

- the storage modulus corresponds to the mechanical energy stored by the material during a stress cycle and is therefore related to the stiffness and shape recovery of the polymer. It can thus be stated that the storage modulus G^I is related to the elastic modulus.
- the loss modulus G^{II} indicates the ability of the polymer to disperse mechanical energy through internal molecular movements. G^{II} represents the damping behavior and is therefore linked to viscosity.

By applying a sinusoidal stress, an ideally elastic material will immediately and completely recover the deformation; therefore, in the case of elasticity, stress and strain will be in phase.
If the material is viscous, the deformation will not be recovered, so that stress and deformation will be out of phase by 90°. Combining the two types of behavior, a viscoelastic material will have a phase lag δ between stress and strain ranging from 0 to 90°.
The equations that relate the phase lag δ expressed in radian, the storage modulus G^I and the loss module G^{II}, both in Pascal, depending on the frequency of strain oscillation are the following:

$$G^I(\omega) = \frac{\tau}{\varepsilon}\cos(\delta) \quad , \tag{2.1}$$

$$G^{II}(\omega) = \frac{\tau}{\varepsilon}\sin(\delta) \quad , \tag{2.2}$$

$$\frac{G^{II}}{G^I} = \tan(\delta) \quad , \tag{2.3}$$

where ω is the frequency of strain oscillation expressed in rad/s, τ is the tangential shear stress in Pascal, ε is the deformation response of the material.
In this study, the dynamic mechanical analysis was performed using a rotational parallel-plate rheometer ARES-RFS (*Rheometrics Fluid Spectrometer*) in torsion (Figure 2.8), available in the Te.Si. laboratories of the Department.

Figure 2.8 *Rotational rheometer ARES-RFS used for mechanical test.*

The sample is placed between two plates and subjected to a rotational oscillatory movement of the lower plate by an electric motor, while the upper plate acts as a detector (Figure 2.9).

Figure 2.9 *Parallel plates of the rotational rheometer with a 10% gelatin methacrylate hydrogel sample: the lower plate is subjected by an electric motor to a rotational oscillatory movement, the upper plate acts as a detector.*

To perform the dynamic mechanical analysis, gelatin methacrylate samples of circular geometry were realized using the 3D printer, with a 3.5 cm diameter and a thickness of about 0.4 mm. After introducing the hydrogel into the extrusion syringe, it was brought to a temperature of 37 °C in a water bath and subsequently cooled in a fridge at 4 °C for different times depending on the GelMA concentration.

The tests were performed on 10% and 13% gelatin methacrylate hydrogel samples, so the 10% GelMA hydrogel was cooled for about 10 minutes, the 13% hydrogel for about 8 minutes because it is clearly more viscous having a higher polymer concentration. The cooling allows to reach the adequate viscosity to perform the printing, since the filament must be neither too liquid to avoid the collapse of the structure or bubbles formation, nor too viscous to allow a regular deposition of bioink from the extruder. Once the necessary cooling time had elapsed, the extrusion syringe, filled with hydrogel, was been loaded onto the 3D bioprinter and the printings have been carried out using a nozzle with a 0.41 mm diameter. The printings were performed on Petri dishes, using a single extruder that supplied the filament at a speed of 6 mm/s; after printing, PBS was added in the Petri dishes containing the samples to keep them hydrated.

The tests were performed in strain-controlled mode at room temperature, about 21 °C, using the rotational rheometer with parallel plates of circular geometry, with a 50 mm diameter and separated by a gap of 0.7 mm. The rotation frequency of the lower plate was set to vary from 0.1 to 100 rad/s, with a displacement ramp of 3%.

2.4.1.1 Data analysis

The data obtained from the dynamic mechanical characterization tests were studied with a statistical analysis using the program *Matlab*, with the aim of verifying the presence of significant differences in the viscosity of the hydrogel samples analyzed for the different concentrations of gelatin methacrylate, i.e. 10% and 13%.
The viscosity η, expressed in Pa·s, has been set as the response variable, while the two GelMA concentrations are the categorical predictor with two levels; the deformation frequency is the continuous predictor, which varies in a range from 0.1 to 100 rad/s.
After verifying the assumption of normality with the Anderson-Darling test in order to satisfy the hypotheses of a one-tailed t-test, it was verified whether the average viscosity of the hydrogel with 10% gelatin methacrylate concentration was lower than the 13% one.
The null hypothesis H_0 and the alternative hypothesis H_1 of the test were therefore set as follows:

- H_0 : mean($\eta^{10\%}$) – mean($\eta^{13\%}$) = 0;
- H_1 : mean($\eta^{10\%}$) – mean($\eta^{13\%}$) < 0.

The choice of H_1 formulation is motivated by the hypothesis that an increase in the concentration of GelMA in the hydrogel results in an increase in viscosity.
A two-way ANOVA analysis was then carried out, to study not only the effect of gelatin methacrylate concentration and strain oscillation frequency on viscosity, but also a possible interaction between the two factors.

2.4.2 Differential Scanning Calorimetry

Another test performed on both the polymer and hydrogels used in this research is differential scanning calorimetry (DSC), which is a thermal analysis method that allows to identify the characteristic temperatures of a polymeric material, including the glass transition T_g, crystallization T_c and melting temperatures T_m.
The relevance of the DSC analysis consists in establishing the optimal processing conditions of a given material and determining the range of use.
This type of calorimetry measures the amount of energy absorbed (endothermic phenomena) or released (exothermic phenomena) from the sample in a continuous heating or cooling process.
The instrument detects the difference in heat flows between two pans, an empty one as a reference, and the other containing the polymeric sample, simultaneously subjected to the same temperature program.
There are two types of DSC analysis: power-compensated DSC in which power supply remains constant and heat-flux DSC in which heat flux remains constant. The first uses instruments composed of two separate heating elements, one for the sample and one for reference; between

them a compensation power is established to keep both elements at the same temperature. This energy is the measure of the enthalpy or thermal capacity variation of the sample with respect to the reference.

In the heat-flux DSC calorimeter (Figure 2.10) used in this research, there is a single furnace in which the sample and the reference are heated or cooled; temperature sensors detect the temperature of each pan, thus measuring the temperature difference between them.

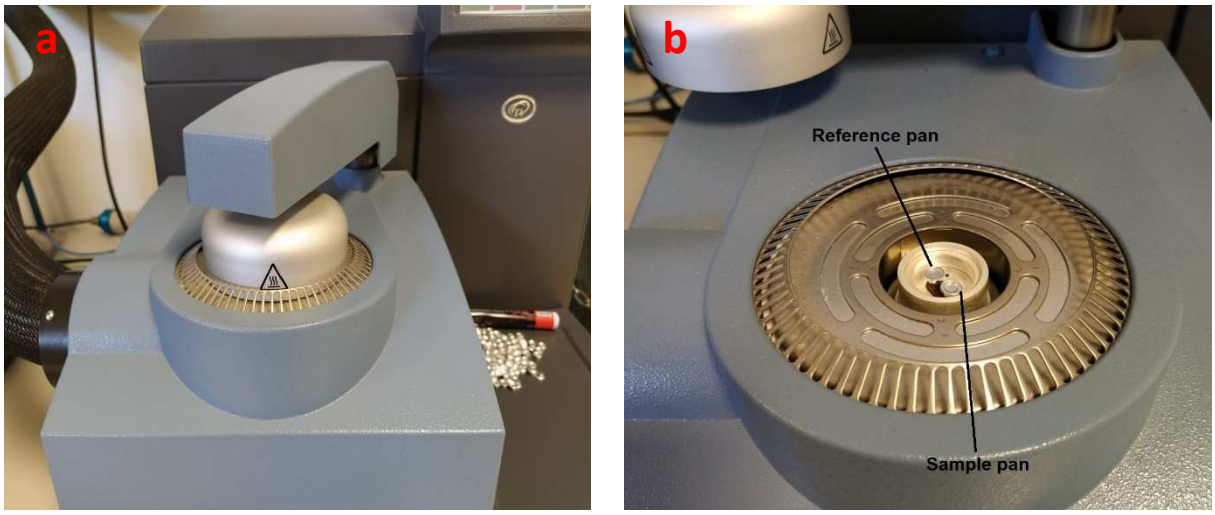

Figure 2.10 *Heat-flux DSC calorimeter (a) showing the positions of reference and sample pans in the single furnace (b).*

The differential scanning calorimetry analysis allows to trace a curve that outlines the trend of the heat flow as a function of temperature, highlighting exothermic and endothermic phenomena. From this curve it is possible to obtain information both on the transitions of the first order, which involve both the latent heat and a specific heat change, including the crystallization and melting temperatures, and on the second-order transitions, which involve only a specific heat change, as the glass transition.

For the DSC analysis 5-10 mg of sample are sufficient; the tests were performed under heating conditions in a temperature range from 0 to 300 °C for the polymer and from 0 to 150 °C for the hydrogels with a 10% and 13% GelMA concentration, with a heating rate of 10 °C/min.

The cooling cycles were not carried out since GelMA is a natural protein-based polymer and, as reported in literature, at these high temperatures it undergoes an irreversible thermal denaturation, thus compromising the possibility of cooling in order to identify a unique crystallization temperature T_c [34].

2.4.3 Swelling property

A test to assess the swelling properties of GelMA-based hydrogels, with concentrations of 10% and 13%, was performed by weighing method.
Ring-shaped molds in polydimethylsiloxane (PDMS) have been produced, with an internal diameter of 8 mm and a height of 4 mm; within each mold a quantity of hydrogel of about 80 µL was placed and 10 replicates were prepared for each analyzed hydrogel concentration.
The samples were placed then under UV light (365 nm) for 60 seconds, after which the molds were removed and the Petri dishes containing the shaped GelMA hydrogels were filled with 3 mL of PBS, in order to cover and keep the whole structure wet; subsequently the hydrogel samples were incubated for 24 hours at 37 °C.
In Figure 2.11, the empty PDMS mold, the mold filled with the un-crosslinked hydrogel, and the final sample are shown.

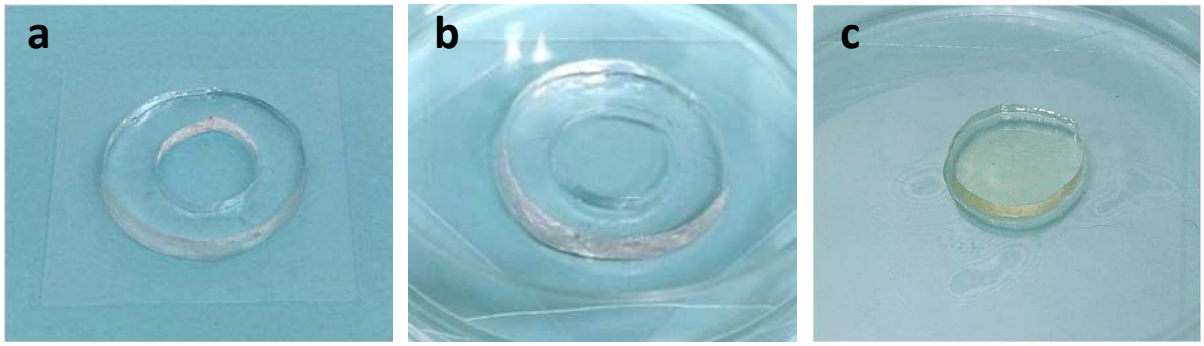

Figure 2.11 *Components of swelling test: (a) empty PDMS mold, (b) mold filled with un-crosslinked hydrogen, (c) final crosslinked GelMA hydrogel sample.*

After this swelling time, the samples were removed from the Petri dishes, dried on its surface with a soft absorbent paper and weighed. They were then let to air-dry for 4 days and ultimately the weight of the samples was recorded by an electronic balance.
The percentage swelling ratio $SR_{\%}$ can be calculated by the following equation [35]:

$$SR_{\%} = \frac{w_w - w_d}{w_w} \cdot 100 \quad , \tag{2.4}$$

with w_w and w_d respectively the wet and the dry weight of the samples.
The swelling properties of hydrogels have a significant impact on the wet shape of samples.
Nichol JW *et al.* (2010) [32] studied the influence of GelMA hydrogel concentration on the swelling ratios, reporting that the $SR_{\%}$ declines with increasing gelatin methacrylate concentration, because of the rise in crosslink densities as GelMA concentration increase.

2.5 Cell tests

Since this research activity involves a biomedical study, the produced hydrogels are loaded with cells before being 3D bioprinted. The types of cells used, and the way in which the experiments are carried out are introduced below.

2.5.1 Cell line

For any cell culture it is necessary to use a growth medium or culture medium, that is a solution freed of all microorganisms by sterilization and containing the substances required for the growth of cells.
The number of available culture mediums is very large and different cell types require a different medium, but it can be said that the culture mediums are basically formed by an isotonic and buffered solution that contains inorganic salts, an energy source such as for example glucose, essential amino acids and other substances, among which the most important is serum or its synthetic analogue; the medium must clearly not contain toxic factors for cells.
The favorable cell environment has a pH of 7.4; the culture media are added with phenol red, which is an indicator that gives qualitative information on the pH of the solution, because it becomes yellow at pH 6.5, is orange at pH 7 and is red at pH 7.6, becoming more purple with increasing pH.
The culture medium, with a certain cell density inside it, is placed in T-flasks, which can be T-25, T-75 or T-150 depending on the size of the culture area, that can be 25 cm^2, 75 cm^2 o 150 cm^2; in general the most used T-flask size during this activity was the T-75 (Figure 2.12).

Figure 2.12 *T-75 flask with culture medium.*

T-flasks for cell culture are stored in an incubator (Figure 2.13) under specific conditions necessary to allow cellular life; the incubator is set at 37 °C with a 21% O_2 and 5% CO_2 internal environment, which are roughly the concentrations of CO_2 and O_2 presents in the human blood, so it is an ideal condition for cell viability and proliferation.

Figure 2.13 *Incubator at 37 °C, with a 21% O_2 and 5% CO_2 internal environment, to cultivate cells.*

When cells proliferate, the surrounding environment tends to acidify, thus leading the medium inside the T-flask to turn into a yellowish color; in this case it will be necessary to aspirate the spent medium, wash the culture area of the T-flask with Hanks' Balanced Salt Solution (HBSS), a saline solution used to keep the osmotic pressure and pH in cells, and replace fresh culture medium into the T-flask (approximately 8 mL for a T-75 flask).
For the first part of the study the interaction of GelMA with human embryonic kidney cells (HEK-293) was analyzed, to get an indication of cell viability after one day.
The culture medium used for HEK-293 is composed about 88% by Dulbecco's Modified Eagle Medium (DMEM), that is a modification of Basal Medium Eagle (BME) that contains four fold concentration of amino acids and vitamins, about 10% by fetal bovine serum (FBS), that is a growth supplement for cell culture media because of its high content of embryonic growth promoting factors, and 1% of both glutamine, which is an essential amino acid required by cultured cells, and penicillin-streptomycin (P/S), that is used to control bacterial contamination.
The experiments aimed at assessing long-term viability and the possible migration of cells within the gelatin methacrylate-based hydrogel instead were carried out using the SK-N-AS cells, that is a type of neuroblastoma cells.
The culture medium of SK-N-AS cells is slightly different from the previous one, because there is the addition of a 1% of Minimal Essential Medium (MEM), which is a synthetic cell culture medium, while the other components respect approximately the same concentrations as the culture medium of HEK-293, because there is about 87% of DMEM, 10% of FBS, 1% of penicillin-streptomycin and 1% of glutamine.

2.5.2 Bioprinting protocol

In order to obtain optimal results, it is essential to operate by sterilizing all the necessary materials so as to avoid undesired contamination; to do so, before each 3D bioprinting test the extruder syringes and the nozzles were subjected to steam sterilization by means of an autoclave that operates at 121 °C and about 1.12 bar (Figure 2.14).

Figure 2.14 *Autoclave for steam sterilization.*

An experiment involving cells seeding within the hydrogel can be performed when cells in culture reach approximately 80-90% confluence (corresponding to surface coverage) within a T-75 flask, so when they are a sufficient quantity for carrying out the test [(36)].
When this condition is reached, it is possible to proceed with the detachment of cells from the surface, on which they deposited and attached during culture, and this procedure involves several steps all carried out under a biological safety cabinet maintaining sterility.
Initially it is necessary to remove the culture medium from the flask, wash the culture surface with HBSS and carry out the trypsinization step, i.e. introduce about 3 mL, if it's a T-75, of trypsin, which is a proteolytic enzyme which breaks down proteins which enable cells to adhere to the flask surface; trypsin is stored at 4 °C and must be heated to 37 °C before use.
The T-flask is then left in incubator at 37 °C for 5 minutes, because trypsin acts at this temperature. At the end of this time, if cells have detached from the surface, the culture medium heated at 37 °C in at least twice the amount of trypsin is added, in order to deactivate trypsin which cannot act too long because otherwise it would break the cell membrane; therefore, about 7 mL of medium are added in a T-75.
The medium and trypsin solution is transferred to a test tube, from which 1 mL is taken and placed in Eppendorf (a test tube with dimensions ranging from 250 µL to 2 mL) in order to perform cell counting. The test tube with 9 mL of solution is placed inside a centrifuge for 5 minutes at 1000 rpm, in order to have a cell pellet deposited at the bottom of it.
Meanwhile, cell counting is performed using a Bürker chamber (Figure 2.15).

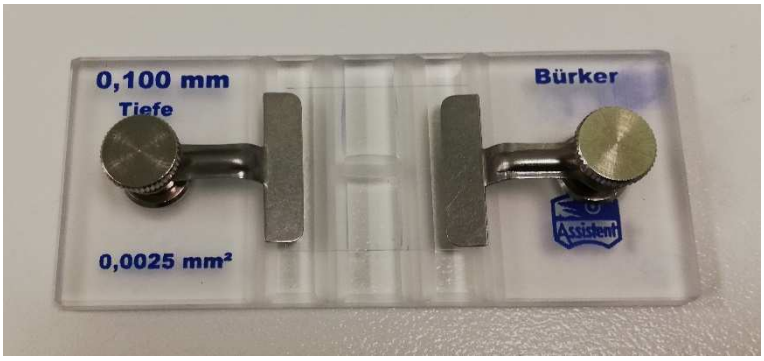

Figure 2.15 *Bürker chamber for cell counting.*

In this process 10 µL of medium with cells are taken from the 1 mL in Eppendorf, and mixed with 10 µL of trypan blue: the latter is a dye capable of assessing cell viability since only dead cells will be marked blue while the live ones will appear bright.
The solution obtained is then placed inside the Bürker chamber which is composed of a grid of nine squares of 1 mm side delimited by three parallel lines, in turn subdivided into sixteen squares each (Figure 2.16).

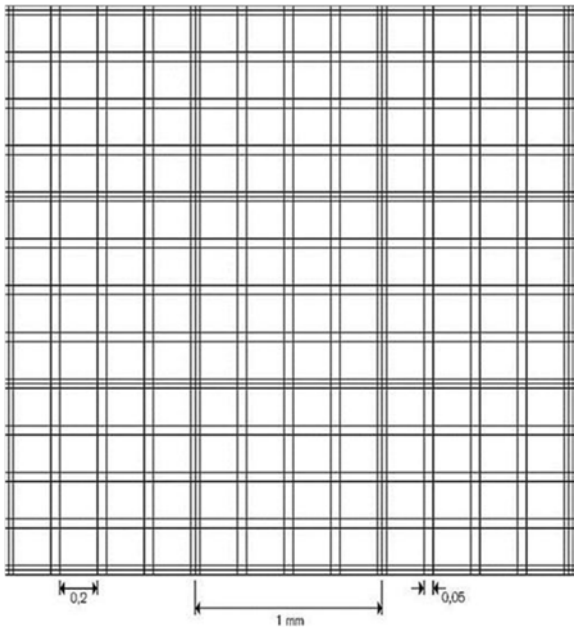

Figure 2.16 *Bürker chamber grid, composed by 9 squares delimited by three parallel lines; each of these is then subdivided into 16 squares.*

Observing under a microscope, cells are counted in at least three squares and then averaged.
The approximate number of cells n_C in the overall culture is obtained by the following equation:

$$n_C = m_C \cdot 2 \cdot 10 \cdot 10^4 \quad , \tag{2.5}$$

where m_C represents the calculated average, 2 derives from the dilution with trypan blue, 10 is the starting solution volume in mL and 10^4 is a corrective factor for the Bürker chamber.
When this centrifuge process is finished and the cell pellet has formed at the bottom of the test tube, medium and trypsin solution is carefully removed and the pellet is resuspended with fresh medium, in a small amount so as not to alter the properties of the hydrogel in which it will be introduced, usually a quantity of medium with an order of magnitude of a few hundred microliters depending on the resulting cells number. A 1:25 is the ideal medium to hydrogel ratio as it results in rather uniform cell suspension and the hydrogel viscosity is not affected [37].
The goal is a density of about 4 million cells per mL of hydrogel, so depending on the available hydrogel volume, the desired amount of medium with cells is taken and is slowly dispersed in GelMA hydrogel, trying to evenly distribute the cells inside it; the hydrogel in which cells are seeded must be taken out of a water bath at 37 °C, because it must be in a liquid state to allow the cellular dispersion.
The remaining part of the medium with dispersed cells is seeded in a new T-flask to continue the cell culture, adding the right amount of fresh medium, i.e. 8 mL if it is a T-75.
When cells have been seeded, the hydrogel is extracted from the test tube and is loaded into an extruder syringe, while another syringe is loaded with hydrogel without cells, if the printing structure involves the use of two extruders.
The extruder syringes are then placed in fridge at 4 °C for a time mainly dependent on the concentration of the hydrogel, usually between 8 and 15 minutes, to allow the sol-gel transition that makes printing possible.
At the end of this cooling process, syringes are placed on their 3D bioprinter seats, as in Figure 2.17.

Figure 2.17 *Extruder syringes loaded on the 3D bioprinter: on the left the one containing the cell-laden hydrogel and on the right the one with the hydrogel without cells; both are GelMA 10% hydrogel.*

At this point in the procedure the 3D bioprinter must be calibrated and, after placing the Petri dish on the printer plate, start printing by choosing the G-Code file of the desired printing structure. At the end of printing, when the structure is formed, it must be exposed to UV radiation to allow the GelMA hydrogel crosslinking; UV exposure times of 30 seconds and 1 minute were assessed in the experiments, not exceeding this value to avoid killing cells.
As last step, culture medium is added in the Petri dish to allow cells to live within the hydrogel and provide them with nutrients; the Petri dish is then stored in the incubator.
The entire detailed protocol for bioprinting is reported below, where the values are given considering a T-75 flask and the passages refer to a printing that involves the use of two extruders simultaneously:

- trypsin, culture medium and two test tubes with the same hydrogel placed in water bath at 37 °C;
- remove medium from the flask and wash culture surface with HBSS;
- remove HBSS and place 3 mL of trypsin in the flask;
- flask with trypsin in incubator at 37 °C for 5 minutes;
- place 7 mL of culture medium in the flask or at least twice the amount of trypsin;
- transfer the solution in a test tube, from which 1 mL is removed and placed in Eppendorf;
- test tube with 9 mL of solution in centrifuge for 5 min at 1000 rpm;
- withdraw 10 μL of solution from the Eppendorf and, after mixing with 10 μL of trypan blue, fill the Bürker chamber for cell counting;
- remove 9 mL of solution and resuspend cell pellet in about 400 μL (or a multiple of 200 μL);
- withdraw a quantity of solution so that approximately 4 million cells per mL of hydrogel can be seeded; remaining solution transferred to a new flask, in addition to 8 mL of medium, to continue cell culture;
- disperse medium with cells in a hydrogel and mix slowly by hand;
- take cell-laden hydrogel and load it into an extruder; the same for the other hydrogel;
- extruders in fridge at 4 °C for a time to be defined, in order to carry out the sol-gel transition of the hydrogel;
- place extruders on the 3D bioprinter and calibrate it;
- carry out the desired printing;
- UV exposure for a maximum of 1 min to crosslink the hydrogel;
- add culture medium in the Petri dish and store it in incubator at 37 °C.

2.5.3 Experiments

In the biological validation experiments performed, some parameters were changed in order to identify the ideal conditions, such as the concentration of gelatin methacrylate in the hydrogel, the time of exposure to UV radiation, the type of cell line seeded in the hydrogel, the printing structure, the cellular density inside the hydrogel.
The following table summarizes the specifications of each experiment:

Table 2.1 *Specifications of each experiment performed, pointing out which ones will be analyzed in the evaluation of the results.*

Experiment number	Concentration [%]	UV exposure time [s]	cells / hydrogel [mln / mL]	Structure design	Cell population	Present in results
1	10	30	3	Three chambers	HEK-293	✓
2	10	30	3.5	6 channels ladder	SK-N-AS	×
3	10	30	4	8 channels ladder	SK-N-AS	✓
4	10	60	2.5	6 channels ladder	SK-N-AS	✓
5	13	30	3.25	8 channels ladder	SK-N-AS	✓
6	13	60	5	8 channels ladder	SK-N-AS	×
7	13	60	5	8 channels ladder	SK-N-AS + exosomes	✓
8	13	60	5.75	8 channels ladder	SK-N-AS + exosomes	×
9	13	60	4	8 channels ladder	SK-N-AS + exosomes	×

2.5.4 Evaluation of cell viability

Once bioprinted, it is possible to study the cell viability within the hydrogel scaffold.
To do this, a live/dead fluorescence test is used, which can provide a quick method to evaluate the portion of live and dead cells.
Cell viability, as seen for cell counting, is determined using fluorescent dyes; those used in this research are based on calcein acetoxymethyl ester (calcein-AM), propidium iodide (PI) and Hoechst 33258.
Calcein-AM (Figure 2.18) itself is not fluorescent, but it is permeable to membranes and is able to penetrate inside living cells to produce an intense and uniform green fluorescence.

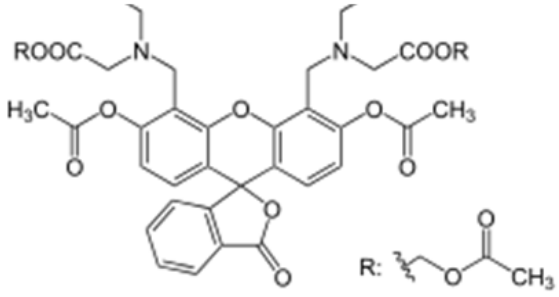

Figure 2.18 *Chemical structure of calcein-AM.*

Propidium iodide (Figure 2.19), on the other hand, can only pass through damaged membranes and undergo a fluorescence increase of 20-30 times after binding to nucleic acids, thus producing a bright red fluorescence in dead cells [38].

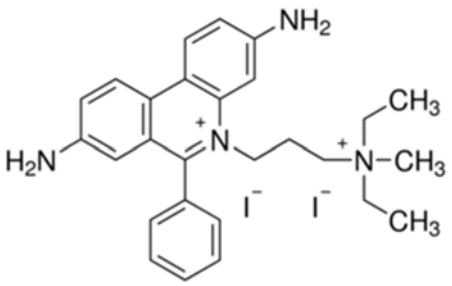

Figure 2.19 *Chemical structure of propidium iodide.*

Hoechst 33258 (Figure 2.20) is a cell-permeant nuclear counterstain that emits blue fluorescence when bound to DNA, then in the performed experiments it has the function to mark all the cells present inside the bioprinted hydrogel.

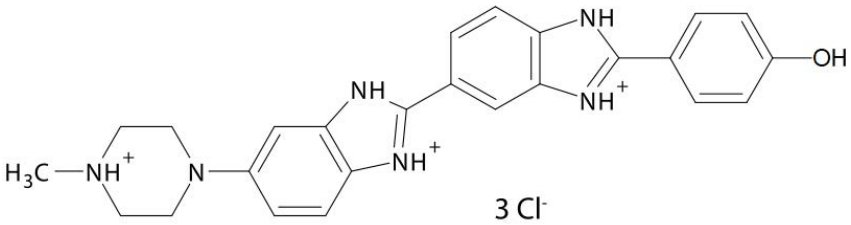

Figure 2.20 *Chemical structure of Hoechst 33258.*

To perform fluorescence tests a staining solution consisting of 1 µL calcein-AM, 5 µL PI and 1 µL Hoechst 33258 per mL of HBSS is mixed and placed in the Petri dish in which the structure was printed, after elimination of culture medium and washing with HBSS.

It is also possible to carry out an immunofluorescence test without having to terminate the cell culture in the experiment, i.e. an intermediate test after which the staining solution can be removed, and the experiment can be preserved and further carried on. In this case, the solution for the immunofluorescence containing the fluorophores must be prepared in DMEM, not in HBSS, and without the use of propidium iodide because it is toxic and therefore would kill the cells without allowing their culture to continue.

To obtain a numerical indication of cell viability within the tests, an analysis was performed using *ImageJ*, a program in which live and dead cells (if only calcein-AM and propidium iodide were used in the fluorescence test) or live and total cells (if all three substances including

Hoechst 33258 were used in the fluorescence test) were counted from photos saved under a microscope and through the following calculations the percentage viability $v_{\%}$ was obtained:

$$v_{\%} = \frac{live}{live+dead} \cdot 100 \quad , \tag{2.6}$$

$$v_{\%} = \frac{live}{total} \cdot 100 \quad . \tag{2.7}$$

Chapter 3

Experimental results

In this chapter the improvements obtained regarding the optimization of GelMA synthesis and the hydrogel preparation are exposed; the experimental results from the mechanical and cellular tests are then shown.

3.1 Polymer synthesis

As already explained in §2.2, two different methods of synthesis of gelatin methacrylate polymer have been used, which substantially differ only in the purification step aimed at extracting the unreacted methacrylic anhydride and the methacrylic acid formed.
The polymer obtained by the application of the protocol that requires the use of the lyophilizer, was very soft and with an almost spongy structure (Figure 3.1)

Figure 3.1 *Gelatin methacrylate polymer synthesized with the Van Den Bulcke et al. (2000) method that provides dialysis and freeze-drying.*

The GelMA polymer produced with the second method, in which the purification process is carried out by ethanol precipitation, was instead a hard and compact pellet (Figure 3.2).

Figure 3.2 *Gelatin methacrylate polymer synthesized with the Brigo et al. (2017) method that provides precipitation in ethanol and vacuum drying.*

The drying process using a lyophilizer is usually more efficient than the vacuum drying following the precipitation in ethanol, but due to the unavailability of a freeze-dryer it was preferred to proceed with the Brigo *et al.* (2017) method. Furthermore, the hydrogel obtained from GelMA synthesized with the first method was always denatured and not usable for bioprinting applications, unlike the one coming from precipitation in ethanol (Figure 3.3).

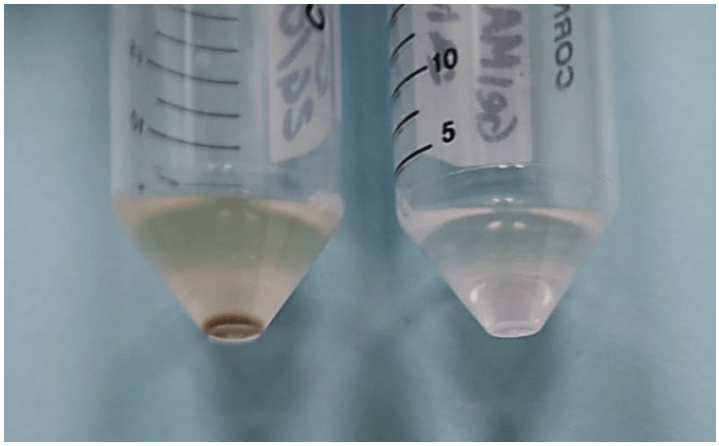

Figure 3.3 *Gelatin methacrylate hydrogel: on the left the one coming from the lyophilized polymer, on the right the one from the polymer precipitated in ethanol.*

Another reason why the use of ethanol is favorable in this work is the fact that ethanol also acts as a sterilizing agent for gelatin methacrylate; sterilization would not be possible, for example, by UV exposure because the polymer would reticulate, preventing its use.

3.2 Optimization of GelMA hydrogel bioprinting

During this activity it was necessary to investigate which were the optimal conditions for different parameters, in order to obtain a good bioprintability and successful experiments.
Among the key parameters on which it was possible to act for this purpose, the main one is the concentration of GelMA in the hydrogel; other important factors were the printing pressure, the size of the nozzles used, the printing speed, the number of layers composing the structure to be printed.

3.2.1 Hydrogel concentration

Four different hydrogels were tested, varying the concentrations of gelatin methacrylate in order to identify some of them with optimal behavior.
It has been noted that, as expected, the viscosity of the hydrogels undergoes a net increase with increasing GelMA concentration; this affects the printability of the hydrogel, making it necessary to use a higher printing pressure. In addition, the hydrogel appears rather grainy.
In parallel, however, with the increase in the concentration of gelatin methacrylate there is a gain in printing accuracy, guaranteeing a better definition.
The tested hydrogels have 5%, 10%, 13% and 15% GelMA concentrations (w/v).
To carry out these tests, the 8 channels ladder (§2.1.2.1) was used as printing structure, using only one extruder, the one that includes the hydrogel without cells inside. This choice was made because this is the part of the structure that requires the most printing precision, since it contains the connection channels, while the cell-laden part would only give partial indications on the printing accuracy, being a simple parallelepiped without any particular detail.
A hydrogel with 5% w/v of gelatin methacrylate is too liquid to be used in a 3D printing application, not guaranteeing a defined and solid structure (Figure 3.4).

Figure 3.4 *Right side of 8 channels ladder structure printed with 5% GelMA hydrogel.*

GelMA hydrogel at 10% instead is quite good as regards the definition of the structure. The channels have a much more accurate shape than those obtained for the 5% concentration (Figure 3.5).

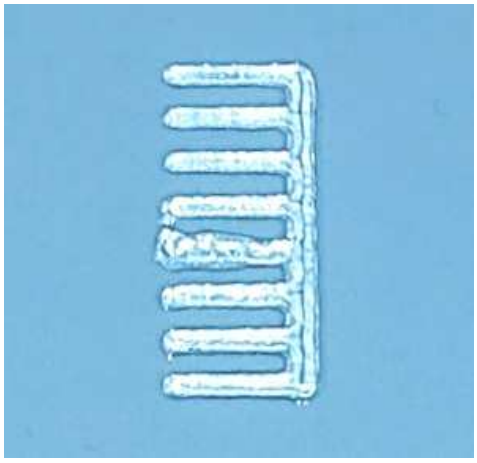

Figure 3.5 *Right side of 8 channels ladder structure printed with 10% GelMA hydrogel.*

The use of a 13% gelatin methacrylate-based hydrogel allowed a good printability of the desired structure, highlighted by the observable precision in the channels, and a hydrogel viscosity suitable for the desired applications (Figure 3.6).

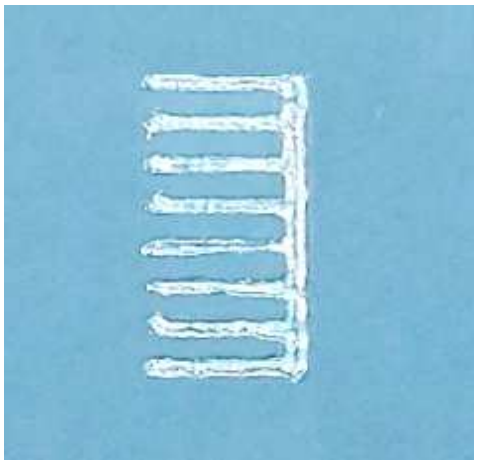

Figure 3.6 *Right side of 8 channels ladder structure printed with 13% GelMA hydrogel.*

The 15% GelMA hydrogel proved to be quite grainy and very viscous, therefore unfavorable for 3D bioprinting. It would also create an unsuitable environment for cell proliferation and too irregular for their movement (Figure 3.7). Nevertheless, this hydrogel was tested in an exploratory cell experiment, proving that lower concentrations were preferable.

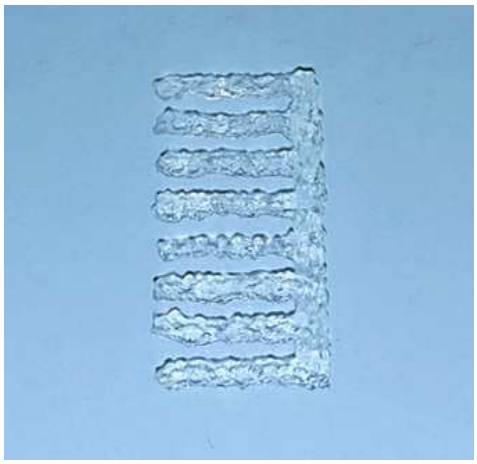

Figure 3.7 *Right side of 8 channels ladder structure printed with 15% GelMA hydrogel.*

These studies led to the identification of the ideal GelMA concentrations for bioprinting, so that 10% and 13% hydrogels were chosen for most of the following experiments carried out during this research.

3.2.2 Parameters

Among the various parameters that can influence the success of the experiments carried out, the **choice of the nozzle** can certainly be considered crucial. In our case, the size used for all the tests carried out was 0.28 mm, so the printed structures were designed with dimensions (in particular the height) compatible to the diameter of this nozzle.
The height of the structures was designed at 0.6 mm; this means that each printing involves the deposition of two overlapping layers of bioink (i.e. hydrogel). The choice of the layers number was made in a very precise manner: the use of a single layer was tested but did not guarantee neither adhesion to the substrate nor a solidity of the structure necessary for its preservation and its study over the days after printing.
A three layers structures, on the other hand, would have been oversized compared to the needs of the experiments performed, since two layers proved to be sufficient to obtain the desired stiffness, adhesion and accuracy. Moreover, with three layers the printing time would be greater, thus risking that the hydrogel undergoes the sol-gel transition during printing, becoming liquid and failing to maintain an adequate viscosity in the extruder.

Another variable that can greatly affect the printing performance is the **printing speed**, that is the speed of movement of the extruders to form the required structure. This was set at 4 mm/s, which proved to be a good compromise between time to print and accuracy. Faster printing speeds could affect correct bioink deposition, resulting in an incomplete structure, with missing

parts. A lower printing speed, on the contrary, in addition to an increase in printing time, would result in a greater accumulation of bioink, creating a filament that can lead to a worse structure definition.

The **cooling time** necessary to obtain the sol-gel transition, and the **printing air pressure** to be supplied to obtain the hydrogel deposition on the substrate, are parameters that depend on many factors. The most important are the concentration of the hydrogel, the temperature of the environment (the laboratory temperature), the total printing time which includes the calibration and formation of the desired structure times, and the cell density (and therefore the quantity of culture medium within the hydrogel). Due to all these factors, cooling time and printing pressure are difficult to predict and should be monitored carefully in each test.
These two parameters undergo small variations according to the different factors mentioned, and a qualitative indication is obtained by doing some tests; for the execution of the printing tests at different hydrogel concentrations shown in §3.2.1, the values of cooling time at 4 °C expressed in minutes and printing pressure in kPa reported in Table 3.1 were obtained.

Table 3.1 *Cooling time to obtain hydrogel sol-gel transition and printing pressure derived from printing tests with different GelMA hydrogel concentrations.*

GelMA concentration [%]	Cooling time [min]	Printing pressure [kPa]
5	14	5
10	12	50
13	12	80
15	10	100

The table shows plausible values, since an increase in gelatin methacrylate concentration in the hydrogel determines a decrease in the time required to obtain the sol-gel transition and an inverse behavior regarding the air pressure to be supplied to the extruders to depose the hydrogel. Printing pressure, as can be seen, undergoes a rather wide variation in the analyzed concentration range.

3.3 Material characterization

The results of the tests performed on the samples are shown below, by means of graphic interpretation and data processing.

3.3.1 Dynamic mechanical analysis

In order to realize the circular samples for the dynamic mechanical characterization, an adjustment of the printing parameters was performed with *Slic3r*, focusing on the infilling pattern of the structure. A concentric geometry infill (Figure 3.8) revealed problems as it leads to voids formation when the nozzle is raised to create the successive concentric circles.

Figure 3.8 *GelMA hydrogel sample with concentric geometry infill: the hydrogel distribution is discontinuous.*

It was therefore convenient to set a rectilinear geometry for the infilling pattern, thus avoiding these problems and obtaining a well-filled structure without voids. (Figure 3.9).

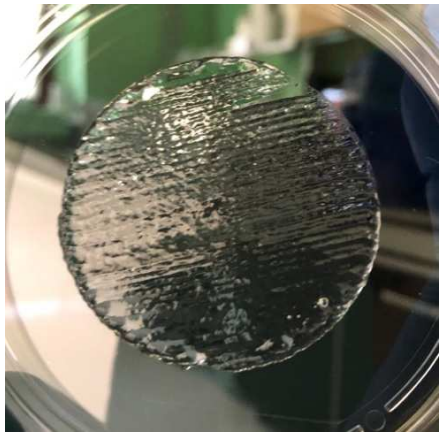

Figure 3.9 *GelMA hydrogel sample with rectilinear geometry infill: the hydrogel distribution is homogeneous.*

Regarding infill densities, those below 20% leads to samples with empty spaces between the filaments, thus presenting discontinuity in the distribution of the hydrogel. The optimal density was chosen at 20%, since higher densities give rise to excessive thicknesses of the sample.
Given the relatively large size of the sample, it was also necessary to adjust the printing speed. The choice was to print at a speed of about 6 mm/s, in order to maintain an adequate viscosity of the hydrogel in the extruder, before it becomes excessively liquid if exposed to ambient temperature for a prolonged time.
A t-test was performed to compare the viscosity of hydrogels with GelMA concentrations at 10% and 13%, giving a p-value of 0.08. The difference in the averages is thus not statistically significant, despite the p-value being just above the limit value of 0.05. This holds true for all deformation frequency values, except the lowest one. It can therefore be stated that, despite the proximity of the p-value to the limit value, it is not possible to reject the null hypothesis H_0 that the averages are equal.
Table 3.2 shows the results of the two-way ANOVA test performed, reporting the two variables analyzed: the GelMA concentration and the deformation frequency, and the product between them. The term *Error* indicates the variation within the groups; *SSE* the sum of square errors; *d.o.f.* the degrees of freedom used to calculate *MSE*, that is the mean square error calculated as the ratio between *SSE* and *d.o.f.*; the *F* factor indicates the ratio between the *MSE* of each variable and the *MSE* of the *Error*. This means that the relationship between the *MSE* among the groups and the *MSE* within the groups is a random variable with the *F* distribution; the higher the value of *F*, the more probable it is that the variability of the group with respect to the others is more relevant than the variability within the groups, i.e. the intrinsic one. The P-value has the function of indicating whether the value of *F* is such as to highlight a statistical significance: if the P-value is less than the threshold value of 0.05, then the factor considered has a statistically significant effect on the response; otherwise, if the P-value is greater than 0.05, the effect may simply be due to chance and cannot be considered statistically significant.

Table 3.2 *Results of the two-way ANOVA test performed through Matlab.*

Source	*SSE*	*d.o.f.*	*MSE*	*F*	P-value
GelMA conc.	5.791e+07	1	5.791e+07	7.54	0.006
Frequency	3.114e+08	1	3.114e+08	40.54	0
GelMA conc.*Frequency	1.529e+07	1	1.529e+07	1.99	0.159
Error	2.112e+09	275	7.681e+06		
Total	2.470e+09	278			

From the two-way ANOVA test (Table 3.2), both the gelatin methacrylate concentration and the deformation frequency seem to have an effect on the viscosity, while an interaction between the two factors does not appear to affect it, since its P-value is greater than the threshold value 0.05.

Therefore, a one-sided left-tail t-test does not reject the null hypothesis of equality between the viscosity means for the two gelatin methacrylate hydrogel concentrations analyzed, while from a two-way ANOVA test an effect of the two factors (GelMA concentration and deformation frequency) on viscosity arises.

As can be seen from Figure 3.10, it is evident that an increase in the gelatin methacrylate concentration from 10% to 13% results in a significant increase in the average viscosity from 1.4 kPa·s to 2.2 kPa·s, while an increase in the deformation frequency entails a modest decrease.

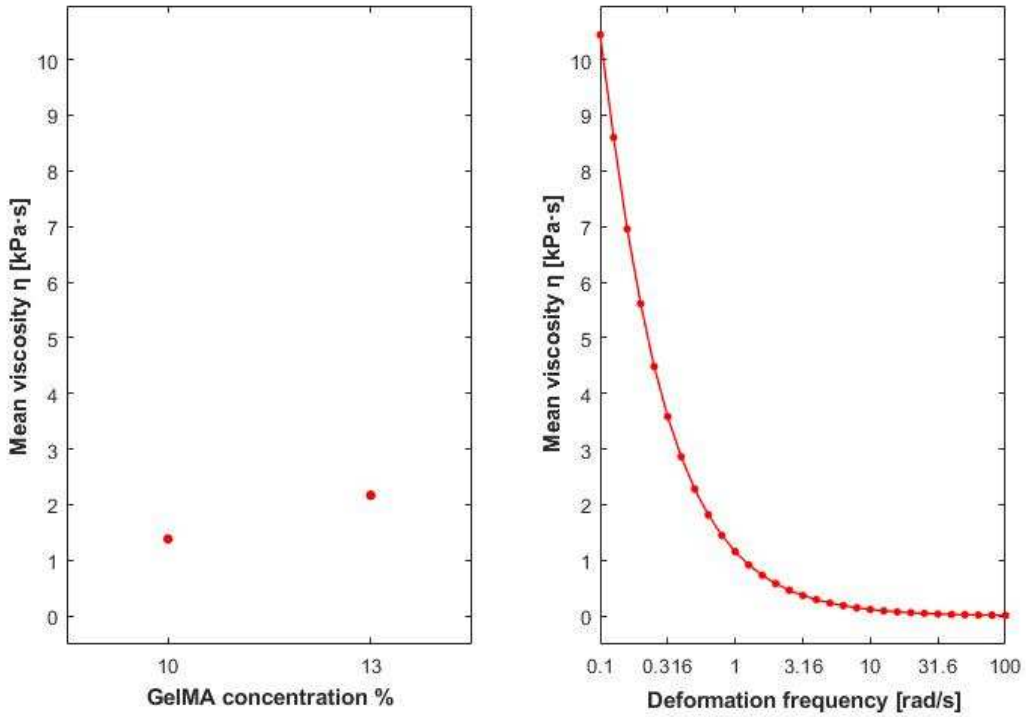

Figure 3.10 *Trend of the mean viscosity as a function of the GelMA concentration on the left and of the deformation frequency on the right.*

3.3.2 Differential Scanning Calorimetry

The DSC test was performed first on the gelatin methacrylate polymer and then on the hydrogels at the different concentrations used in this research, i.e. 10% and 13%.
Four samples of the polymer, synthesized on different days, were analyzed, while two tests were made for the hydrogels at both GelMA concentration of 10% and 13%.
Results obtained from the polymer analysis are consistent and comparable, therefore Figure 3.11 reports only the curve from a single representative sample.

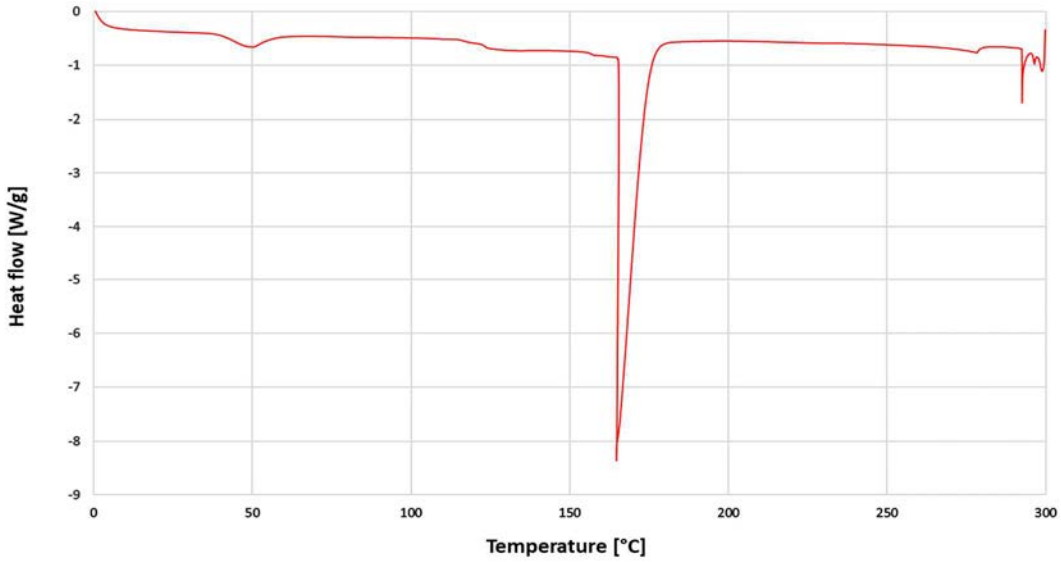

Figure 3.11 *DSC test result on the gelatin methacrylate polymer.*

From the analysis of the data, it was possible to observe that gelatin methacrylate appears to be a partially crystalline polymer, since a very high endothermic peak at 165 °C is seen, which therefore represents the GelMA melting temperature T_m. There is no evidence of the polymer glass transition, and therefore a T_g value is not identifiable.
As mentioned in §2.4.2, cooling cycles were not carried out because of the proteinaceous nature of the polymer, that at high temperatures undergoes an irreversible thermal denaturation. Indeed, the crystallization temperature T_c of the polymer cannot be evaluated univocally.
The tests carried out on the hydrogels also produced consistent results for each analyzed concentration; these are reported in Figure 3.12 and Figure 3.13.

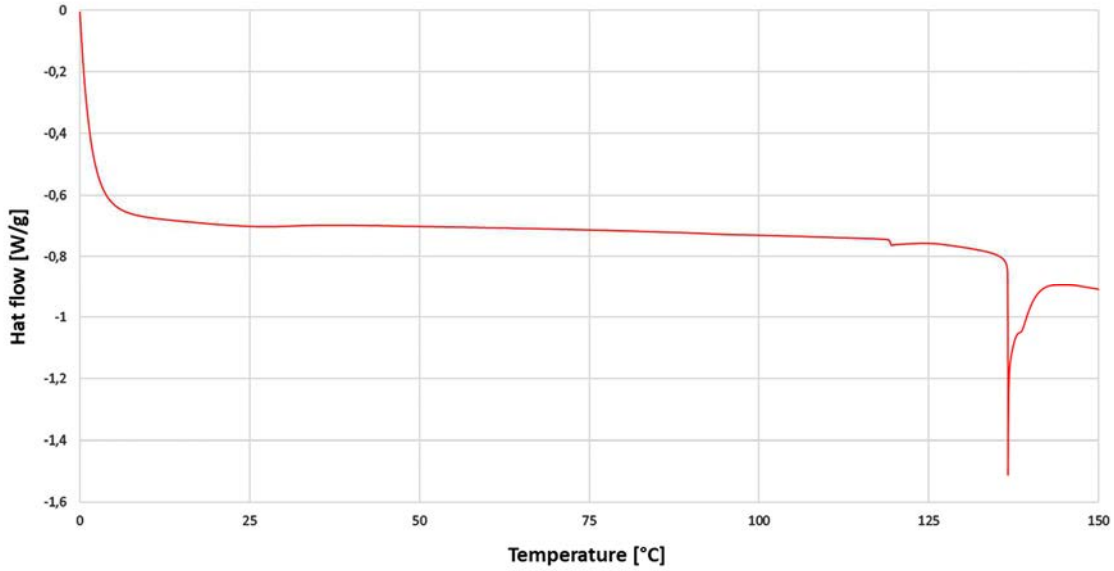

Figure 3.12 *DSC test result on the 10% GelMA hydrogel.*

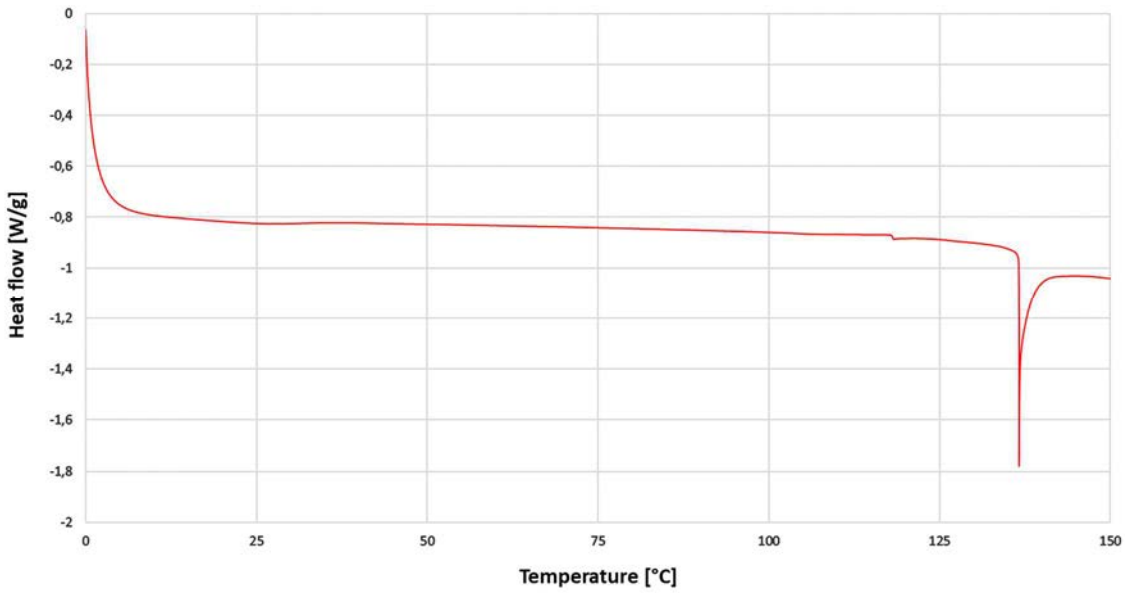

Figure 3.13 *DSC test result on the 13% GelMA hydrogel.*

From data analysis, it was seen that the hydrogels' melting temperatures, highlighted by the endothermic peaks, occur in both cases at lower temperatures with respect to the ones of the pure polymer, and correspond to the value of 137 °C. The T_m shift is justified by the low polymer concentration.

3.3.3 Swelling property

Swelling properties of hydrogels are directly connected to solute diffusion, surface properties, mechanical properties and surface mobility. The swelling ratio of hydrogels depends on the pore size of the polymer network and the interaction between the polymer and the solvent. Particularly, when the hydrogel is used as a scaffold for cell culture, the pore size of the network and the degree of swelling of the polymer indicate the possibility of biological fluids entering and exiting the hydrogel, thus bringing oxygen and nutrients into it, and instead bring to its exterior waste and vesicles released by the cells. Analyzing hydrogel samples at 10% and 13% of concentration it was verified that, maintaining a constant degree of functionalization of the polymer and increasing its concentration, the $SR_{\%}$ decreases, due to the greater crosslinking density. In the case of low concentration variation in the hydrogel, the difference in terms of $SR_{\%}$ is not very high, but still present. Table 3.3 shows the results obtained.

Table 3.3 *Results of the swelling test performed on GelMA hydrogels, showing the percentage swelling ratio and its standard deviation for each concentration.*

GelMA concentration [%]	Swelling ratio [%]	Standard deviation [%]
10	91.59	0.28
13	88.23	0.86

3.4 Cell tests

The experiments shown in Table 2.1 have been performed modifying various parameters in order to determine the ideal conditions.
The main factors that have been modulated are:

- the concentration of GelMA in the hydrogel. The optimized value was established at 13%, after observation of its excellent properties (already discussed in §3.2.1);
- the time of exposure to UV radiation, initially set at 30 seconds to avoid cell damage or killing. It was then observed that even a doubled exposure time did not affect cell viability significantly. 60 seconds of UV exposure have therefore been chosen as the optimized time, given the improved structural stiffness to the printing hydrogel that results from the increased degree of crosslink;
- the cell density within the hydrogel, which depends on the amount of available cells in culture, but with the general goal of using ~4 million cells per mL of hydrogel. At first, HEK-293 were used in viability studies in GelMA hydrogels, while SK-N-AS

neuroblastoma cells were used for all other studies. Moreover, in the last three experiments exosomes were also loaded in the part of the structure without cells, to study if their presence induced any changes in cell behavior observed in previous experiments with cells only;

- the printing structure. For the first experiment we used the three-chambers one, followed by the two ladder structures, preferring the one with eight channels for the reasons already discussed in §2.1.2.

When conditions made it possible, technical replicates were also performed, i.e. more than one printing during the same experiment.

In what follows, we report the most significant results of the key experimental runs, and add all remaining data to the Appendices.

3.4.1 Experiment 1

The experiment in which HEK-293 cells and the three-chamber structure were used was aimed at studying their biocompatibility and viability in the hydrogel after 24 hours, using the staining solution comprising calcein-AM (marking live cells in green) and propidium iodide (staining nuclei of dead cells in red) (Figure 3.14).

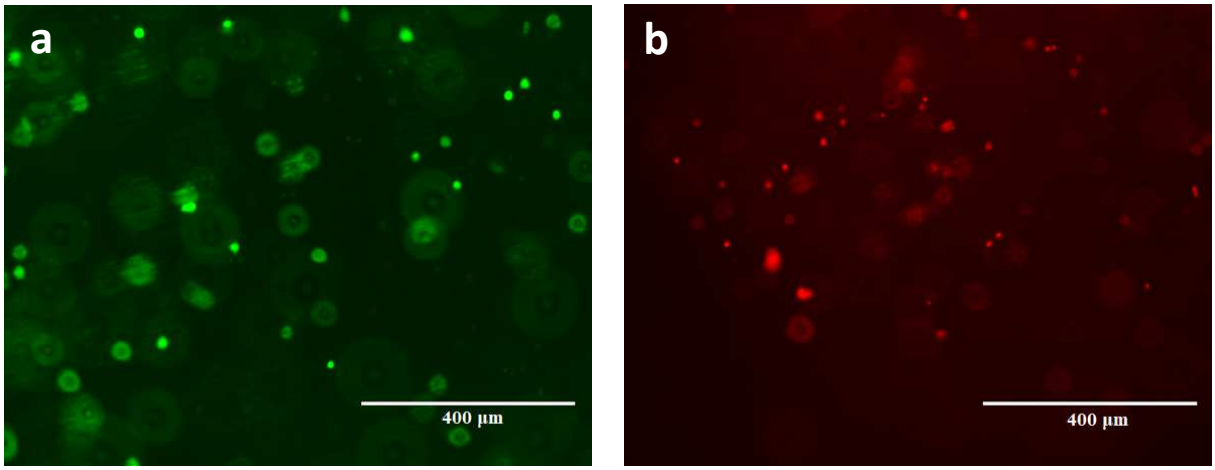

Figure 3.14 *Immunofluorescence test on experiment 1 after 24 hours: a) live cells marked in green by calcein-AM, b) dead cells marked in red by propidium iodide; 10X magnification.*

The immunofluorescence test one day after printing shows that most cells are alive, but also highlights significant numbers of dead cells. Overall, this test gave good signals of cell viability within bioprinted GelMA hydrogels.

3.4.2 Experiment 3

The third experiment involves the use of a 10% GelMA-based hydrogel and, for the first time, the printing of the 8 channels ladder structure. This structure was successfully bioprinted, with excellent definition and consistency of the hydrogel (Figure 3.15), which allowed culture and continuous study for several days after printing.

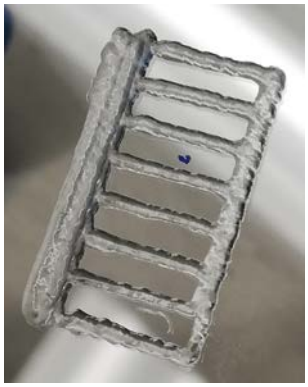

Figure 3.15 *8 channels ladder structure bioprinted with 10% gelatin methacrylate hydrogel.*

In this case, cell culture was maintained until day 7 after printing, and then stopped to evaluate cell viability by using a staining solution that includes all three fluorophores mentioned in §2.5.4, therefore Hoechst 33258 (marking all cells nuclei in blue), calcein-AM and propidium iodide (Figure 3.16).

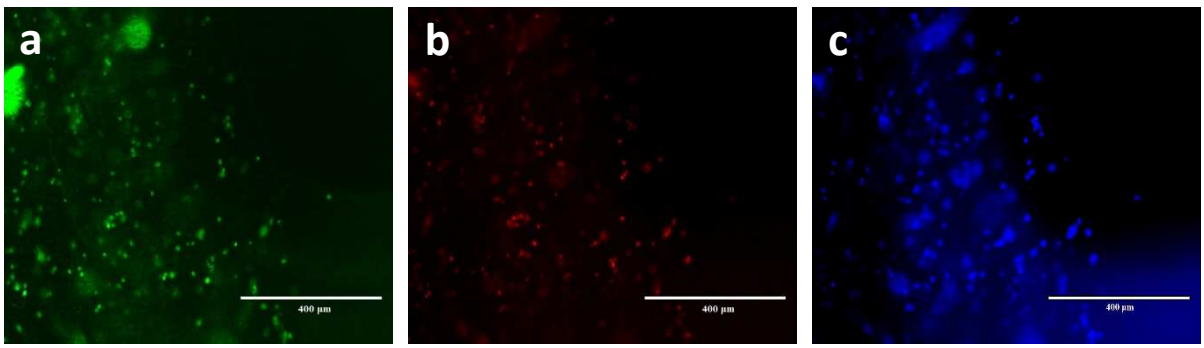

Figure 3.16 *Immunofluorescence test on experiment 3 after 7 days: a) live cells marked in green by calcein-AM, b) dead cells marked in red by propidium iodide, c) total cells marked in blue by Hoechst 33258; 10X magnification.*

As can be seen, cellular viability is rather sustained, since cells marked in green are clearly in a higher quantity than those dead, highlighted in red. Quantitatively, using equations (2.6) and (2.7) in at least three images of this test, a cell viability of about 70% at day 7 can be obtained.

However, from these images it can be observed that spontaneous cell migration is practically nil, since no cell is observed at the entrance to the channels, in the hydrogel originally without cells shown in the lower right corner in each of the three images in Figure 3.16.

3.4.3 Experiment 4

In this experiment the exposure time to UV radiation was doubled (60 seconds), to obtain a greater crosslinking and to investigate whether cell viability was particularly affected.
The cell density in this test was the lowest of all the experiments, around 2.5 million per mL of hydrogel, because at that time the cell culture did not allow to have a higher cells quantity that could guarantee the desired cellular density, i.e. about 4 million per mL of hydrogel.
Another different parameter in this test was the choice of the printing structure, which was the 6 channels ladder, later abandoned for the reasons already explained.
The greater crosslinking gave the hydrogel improved structural strength and stiffness, which allowed to reach day 14 from the moment of printing to carry out the immunofluorescence viability test with the three fluorophores markers described above. Below are shown a bright field microscope image of one of the channels (Figure 3.17), and the same area following the immunofluorescence test (Figure 3.18).

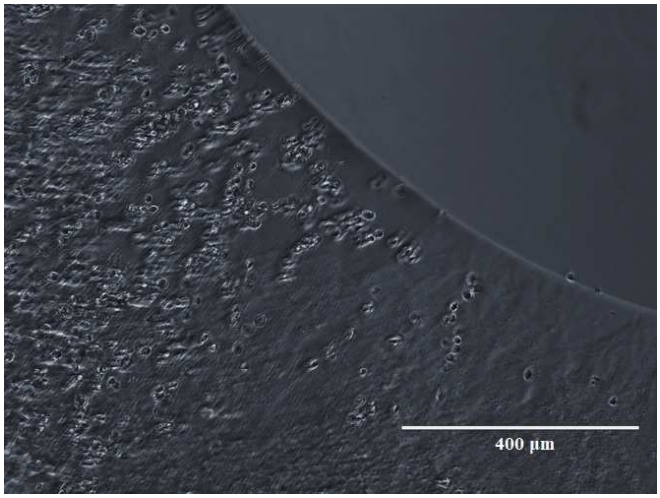

Figure 3.17 *Beginning of a channel of the 6 channels ladder structure in the experiment 4 seen on optical microscopy, in which the SK-N-AS tumor cells are observed; 10X magnification*

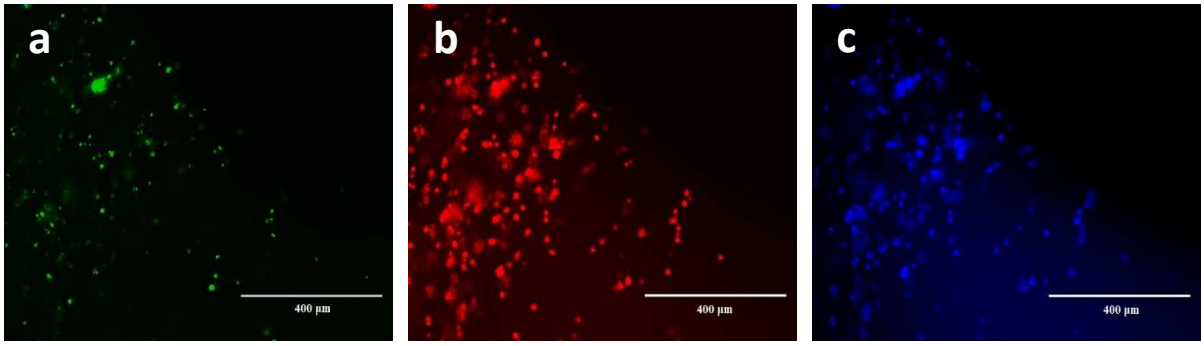

Figure 3.18 *Immunofluorescence test on experiment 4 after 14 days: a) live cells marked in green by calcein-AM, b) dead cells marked in red by propidium iodide, c) total cells marked in blue by Hoechst 33258; 10X magnification.*

In this experiment, cell migration may seem to have begun, because some isolated cells are observed in the initial part of the channel (Figure 3.17), but this equivocal result is explainable by the fact that, during printing, the extruder containing the hydrogel without loaded cells could have slightly dragged a small amount of cell-laden hydrogel, which is almost inevitable since the two parts of the structure printed by two different extruders must have a contact surface in order to analyze the possible cell migration.
In this test, cell viability is clearly lower than that in previous experiments, but this decrease can certainly be linked to the doubled culture time in the hydrogel (14 vs 7 days). In particular, in this case viability was between 30 and 35%, which however is a good result considering the very high culture time. This result also proves that the test was carried out in excellent sterility conditions, since no contamination was found.

3.4.4 Experiment 5

The fifth experiment was the first in which the 13% gelatin methacrylate hydrogel was used, which from then on was the mainly employed hydrogel.
In this experiment, the cell density is higher than that of the previous test, but still slightly less than the desired reference density. In this case about 3.25 million cells were seeded per mL of GelMA hydrogel.
The hydrogel crosslinking in this test was carried out through a 30-second UV exposure, and consequently the experiment was interrupted to analyze its vitality 6 days from printing, before complete structure loss, thus failing to carry on culture until day 14.
The immunofluorescence test in this experiment was performed using a staining solution containing only calcein-AM and propidium iodide. Taking as a reference one of the channels of the 8 channels ladder structure (Figure 3.19), the number of live and dead cells (Figure 3.20) were observed in order to obtain indications on cell viability.

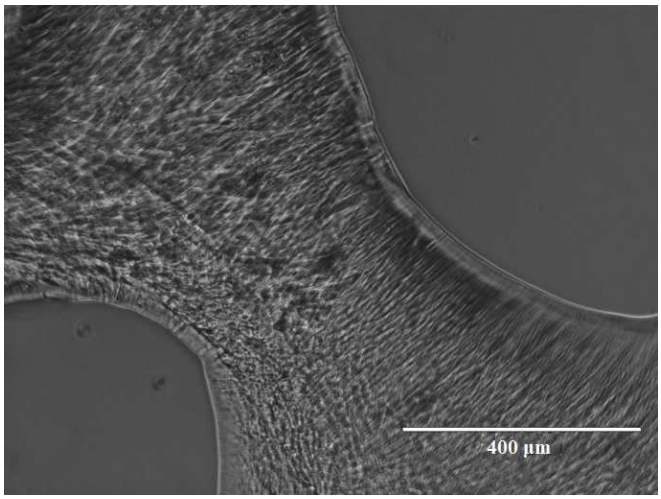

Figure 3.19 *Beginning of a channel of the 8 channels ladder structure in the experiment 5 seen on optical microscopy; 10X magnification.*

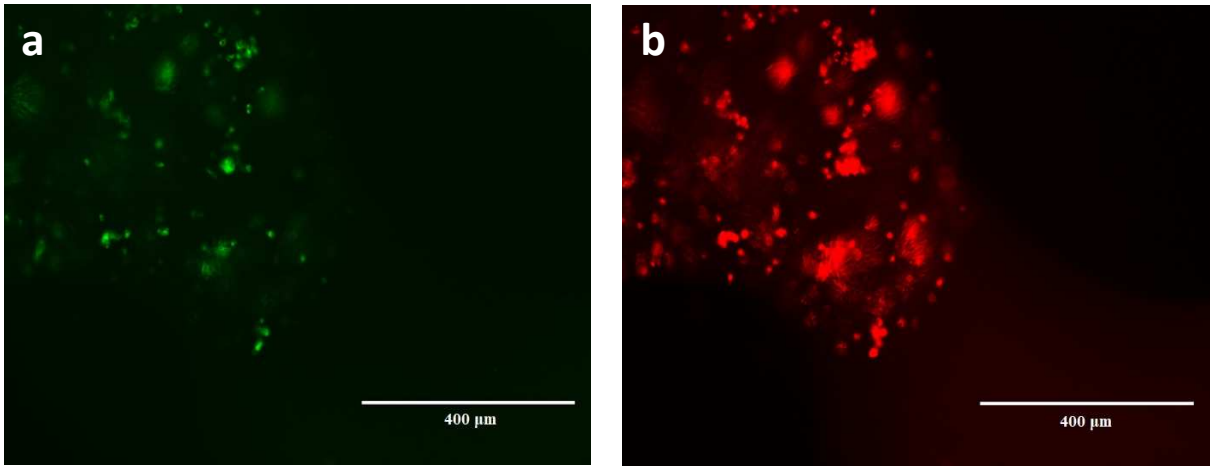

Figure 3.20 *Immunofluorescence test on experiment 5 after 6 days: a) live cells marked in green by calcein-AM, b) dead cells marked in red by propidium iodide; 10X magnification.*

In Figure 3.19 it can be noticed how the tumor cells seeded within the hydrogel are not identifiable as clearly and easily as in the previous case (Figure 3.17), this is because the concentration of gelatin methacrylate in the hydrogel is greater, 13% versus 10% of the fourth experiment, and a greater concentration results in greater stiffness, also limiting visibility under the microscope within the bioprinted structure. Regardless of the difficult identification of cells, it can be observed that even in this experiment, cellular migration inside the hydrogel is null.
As observed in Figure 3.20, the viability of SK-N-AS tumor cells is not very high, since cells marked in red by propidium iodide are in a rather higher quantity than those marked in green by calcein-AM. After quantification, the percentage viability is only around 30%, a value very similar to that of experiment 4 where, however, the immunofluorescence test was done 14 days after printing, so eight days later with respect to this experiment.

3.4.5 Experiment 7

The experiment that produced the most important and promising results was the seventh, in which the main parameters such as UV exposure time, hydrogel concentration and printing structure were already optimized and were respectively: 60 seconds of exposure, 13% of GelMA in the hydrogel and the 8 channels ladder structure.
A variable that, as mentioned, is very difficult to keep constant in each experiment is the density of SK-N-AS cells seeded within the hydrogel, which in this case was 5 million per milliliter of hydrogel.
In this experiment there is an important variant with respect to all previous tests: the presence of exosomes (described in §1.4.2) seeded in the hydrogel without cells. Considering the 8 channels ladder structure, the exosomes are on the right side, in the less wide parallelepiped and the channels.
The reason why the exosomes have been seeded in the hydrogel is that we want to better understand what role they have in the development of a tumor, since preliminary evidence can be found in the literature, and in particular in tumorigenesis induction, tumor growth, metastasis and angiogenesis [39]. In particular, the goal in this research project was to assess whether and how exosomes influence cell clustering and cell migration, therefore if they act as chemoattractants, i.e. substances that, having a chemotactic inducer, have a positive effect on cell motility.
The density of seeded exosomes was approximately 35 μg per mL of hydrogel, and the exosomes were previously marked in red for greater ease of detection, having very small dimensions ranging from 50 to 100 nm.
Since the seeded exosomes expressed a red fluorescent signal, it was not possible to add propidium iodide to mark dead cells in the immunofluorescence test, so only calcein-AM was used. The viability test was carried out three days after the printing.
In this test two technical replicates were bioprinted, so the results are shown for both printings (Figure 3.21); the position of the exosomes marked in red is also observed (Figure 3.22).

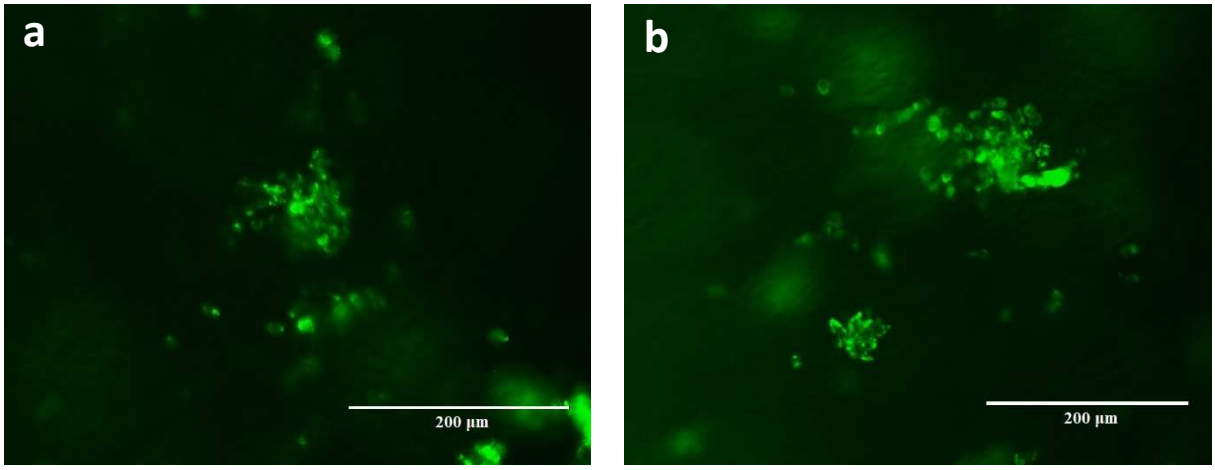

Figure 3.21 *Immunofluorescence test with only calcein-AM on experiment 7 after 3 days: a) first technical replicate, b) second technical replicate; 20X magnification.*

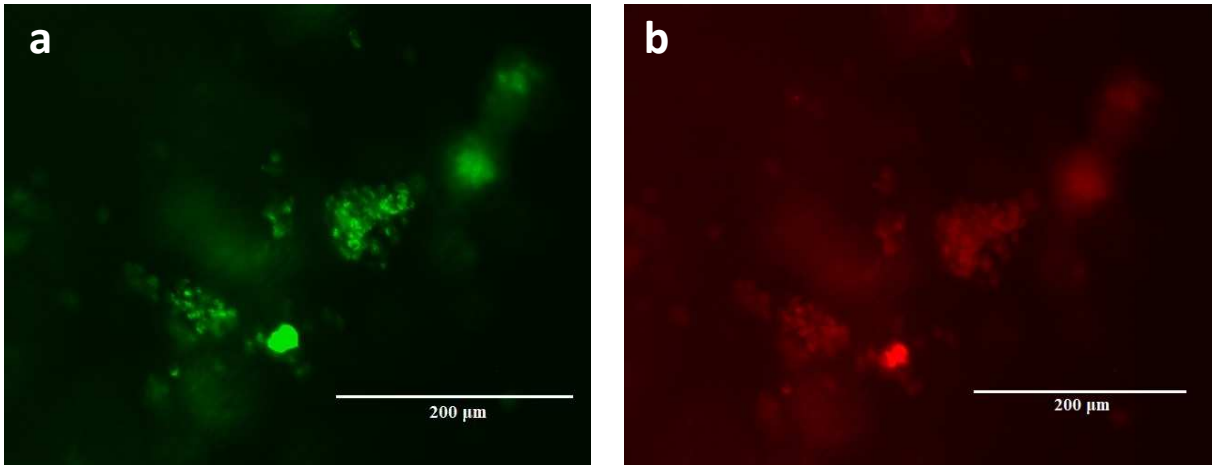

Figure 3.22 *Second technical replicate of experiment 7 after 3 days: a) live cells marked in green by calcein-AM, b) exosomes marked in red; 20X magnification.*

As can be seen in Figure 3.21, cell agglomerates have formed and this could be caused by the presence of exosomes since in previous experiments where only tumor cells were seeded within the hydrogel this phenomenon had never happened. In fact, as confirmed by Figure 3.22, we can observe how the exosomes have been internalized by the cells. This result could mean that, although no evidences of spontaneous cell migration are observed, an induced cell migration occurs due to the presence of exosomes in the environment, which cause the formation of clusters allowing a movement of the cells within the hydrogel in which they are seeded, thus confirming the important role that exosomes play in tumor development.

Chapter 4

Conclusion and future developments

The work carried out in this thesis is the synthesis, optimization and 3D bioprinting of a gelatin methacrylate-based hydrogel, which allows cell culture studies.

The synthesis of the polymer, carried out using two different drying methods, allowed us to optimize the gelatin methacrylate preparation in such a way as to obtain a pure product. The best drying method was the precipitation of the synthesis solution in ethanol with subsequent vacuum drying, while problems were encountered with the purification of the polymer by dialysis with membranes and lyophilization.

This polymer was used for the preparation of the hydrogel, dissolving it in PBS and with the addition of a photoinitiator. Different concentrations of gelatin methacrylate were tested so to obtain hydrogels with an optimal stiffness and viscosity for 3D bioprinting and for subsequent studies. The results define the optimal hydrogels as those with a GelMA concentration of 10% and 13%, since higher concentrations result in too granular and rigid hydrogels, while lower concentrations lead to too liquid and scarcely viscous bioinks.

The design of the printing structures was then carried out, evaluating different geometries in order to select the best one for biological validation and for cell migration studies.

At first, a three-chamber structure was used for a study of cell viability and biocompatibility within the GelMA hydrogel, to be then replaced by an optimized ladder-shaped structure with 8 channels with a 0.5 mm thickness, preferred over the 6 channels version for its easier microscopic observation.

The polymeric material and the hydrogel were then subjected to several tests in order to characterization them and gather information on: *i.* the hydrogel viscosity relating it to its bioprintability, obtaining a higher viscosity for the hydrogel at 13% compared to 10%, as expected; *ii.* the melting temperatures of both the polymer and the hydrogel, showing that a polymer dilution in a solvent moves the melting temperature to a lower value with respect the pure polymer one; *iii.* indications concerning the swelling ratio, which decreases as the concentration of gelatin methacrylate within the hydrogel increases.

When cell culture allowed to have a high number of Neuroblastoma cells, it has been possible to carry out biological tests seeding cells inside the hydrogel, which, together with the same hydrogel but without cells, was printed to obtain the desired 3D structure and to study cell viability and migration. In this research project, nine cellular experiments were carried out, in which by varying the various parameters it was possible to identify the following optimal

factors: *i.* a hydrogel concentration of 10% or 13%, *ii.* a 60 seconds UV exposure in order to crosslink the hydrogel after printing, *iii.* a cell density of about 4 million cells per mL of GelMA hydrogel. The last three experiments were carried out by also introducing exosomes derived from Neuroblastoma cells in the bioink, resulting in significant and promising results concerning the formation of cell clusters following the internalization of exosomes after three days from the printing. This proves the role of exosomes cause in inducing cells migration, a key aspect of tumor growth and metastatic dissemination, while spontaneous cell migration was not observed in any other test.

During the period of this research, some problems were encountered with the 3D bioprinter in the calibration and movement of the extruders, which negatively affected the success of the tests, so for a period it was not possible to carry out biological experiments.

A possible future development could be the further improvement of polymer purification by dialysis with membranes and lyophilization, trying to eliminate the problems encountered and in order to obtain a polymer with a degree of total purity.

A further development could be represented by the use of a 3D bioprinter that can maintain the desired temperature of the extruder, and therefore of the hydrogel, during printing, thus allowing to form structures of greater dimensions or in greater numbers keeping the hydrogel at the ideal consistency and viscosity.

Following the optimization of polymer and hydrogel synthesis and the results obtained in this thesis work, it is possible to continue the study by focusing on the use of exosomes in biological tests, further developing the understanding of the role that these extracellular vesicles have in the metastases proliferation of this tumor.

Another future project on which it will be possible to work is the 3D bioprinting in series of smaller structures inside multiwell culture plates and use hydrogels with different cellular densities inside them.

As regards the tests aimed at characterizing the material used, DSC analysis on the pure polymer can be performed with a cooling cycle in order to have further confirmation of the impossibility of determining the polymer T_c univocally.

It could be useful then to carry out a thermogravimetric analysis (TGA) in order to verify the actual composition of the polymer, so as to identify the possible presence of impurities that can affect the DSC results.

A further development is represented by the execution of other tests on gelatin methacrylate as a Fourier-transform infrared spectroscopy (FTIR) in order to obtain information on the GelMA characteristic groups and a hydrogen-1 nuclear magnetic resonance (H-NMR) to have greater confirmations with respect to the degree of functionalization of the polymer.

Nomenclature

Roman symbols

$d.o.f.$	=	degrees of freedom [-]
E^I	=	storage modulus with axial stress [Pa]
E^{II}	=	loss modulus with axial stress [Pa]
F	=	Fisher factor in ANOVA test [-]
G^I	=	storage modulus with shear stress [Pa]
G^{II}	=	loss modulus with shear stress [Pa]
$\hat{h}$	=	Planck constant [J·s]
H_0	=	null hypothesis of t-test [-]
H_1	=	alternative hypothesis of t-test [-]
m_c	=	mean number of cells [cells/square]
MSE	=	mean square error [-]
n_c	=	approximate number of cells [cells]
$SR_{\%}$	=	percentage swelling ratio [-]
SSE	=	sum of square errors [-]
T_c	=	crystallization temperature [°C]
T_g	=	glass transition temperature [°C]
T_m	=	melting temperature [°C]
$v_{\%}$	=	percentage viability [-]
w_d	=	dry weight [g]
w_w	=	wet weight [g]

Greek symbols

δ	=	damping factor [rad]
ε	=	strain [-]

η	=	hydrogel viscosity [Pa·s]
υ	=	frequency [s^{-1}]
τ	=	tangential shear stress [Pa]
ω	=	frequency of strain oscillation [rad/s]

Acronyms

2D, 3D	=	2- and 3-dimensional
AM	=	acetoxymethyl
BME	=	Basal Medium Eagle
CAD	=	computer-aided design
DMEM	=	Dulbecco's Modified Eagle Medium
DMA	=	dynamic mechanical analysis
DNA	=	deoxyribonucleic acid
DSC	=	differential scanning calorimetry
ECM	=	extracellular matrix
FBS	=	fetal bovine serum
FTIR	=	Fourier-transform infrared spectroscopy
GelMA	=	gelatin methacrylate
HBSS	=	Hanks' Balanced Salt Solution
H-NMR	=	hydrogen-1 nuclear magnetic resonance
MAA	=	methacrylic anhydride
MEM	=	Minimal Essential Medium
MWCO	=	molecular weight cut-off
NB	=	Neuroblastoma
PBS	=	phosphate buffered saline
PDMS	=	polydimethylsiloxane
PEG	=	polyethylene glycol
PEG-DA	=	diacrylate polyethylene glycol
PEG-MA	=	methacrylate polyethylene glycol

pHEMA	=	poly-hydroxyethylmethacrylate
PI	=	propidium iodide
P/S	=	penicillin-streptomycin
TGA	=	thermogravimetric analysis
STL	=	Stereo Lithography
TM	=	trademark
UV	=	ultraviolet
w/v	=	weight/volume

Appendix

A.1 Additional cell tests results

The following figures show the results of other cell experiments not yet shown; they presented problems concerning either the 3D bioprinting or the immunofluorescence test, due to a probable non-complete permeation of the fluorophore dyes.

A.1.1 Experiment 2

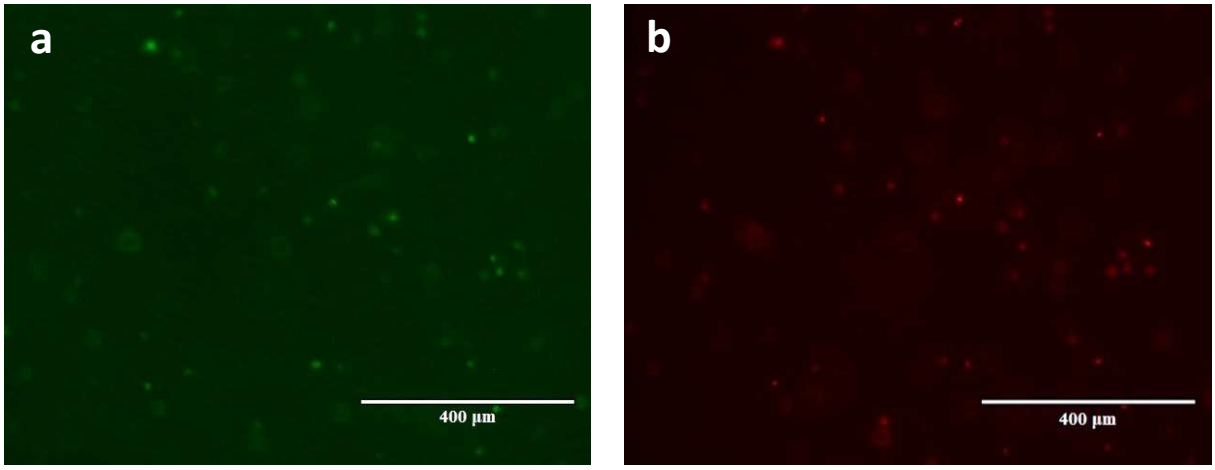

Figure A.1 *Immunofluorescence test on experiment 2 after 3 days: a) live cells marked in green by calcein-AM, b) dead cells marked in red by propidium iodide; 10X magnification.*

A.1.2 Experiment 6

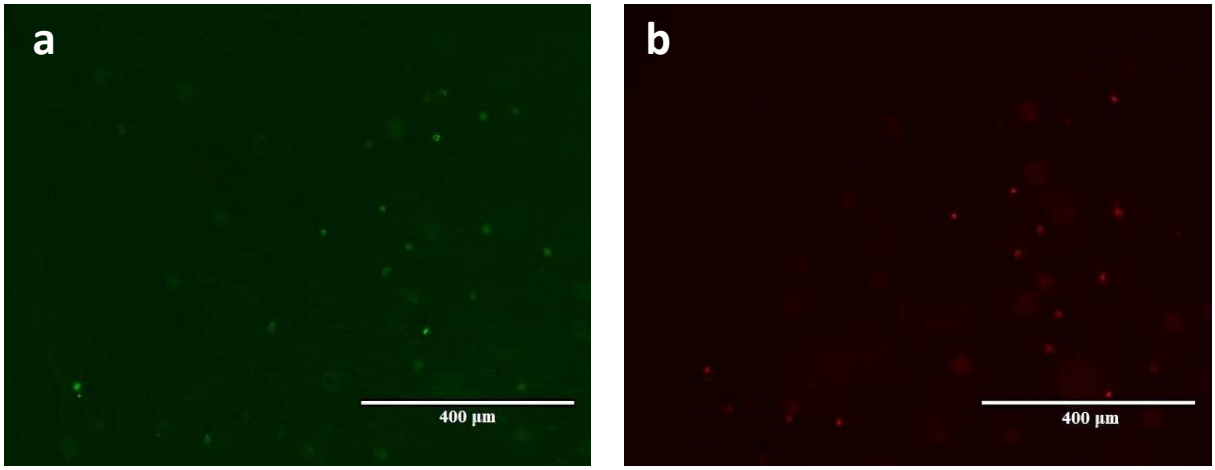

Figure A.2 *Immunofluorescence test on experiment 6 after 7 days: a) live cells marked in green by calcein-AM, b) dead cells marked in red by propidium iodide; 10X magnification.*

A.1.3 Experiment 8

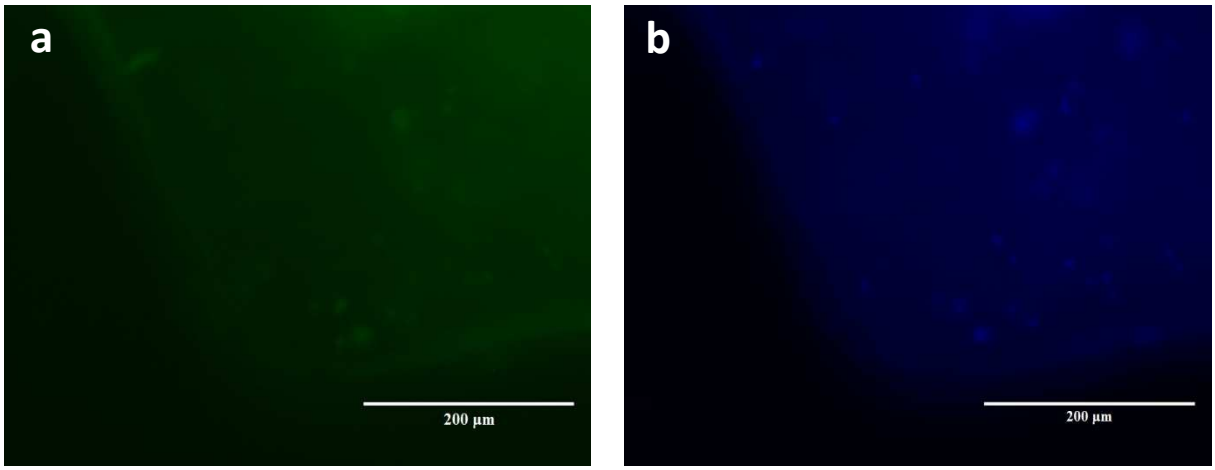

Figure A.3 *Immunofluorescence test on experiment 8 after 14 days: a) live cells marked in green by calcein-AM, b) total cells marked in blue by Hoechst 33258; 20X magnification.*

A.1.4 Experiment 9

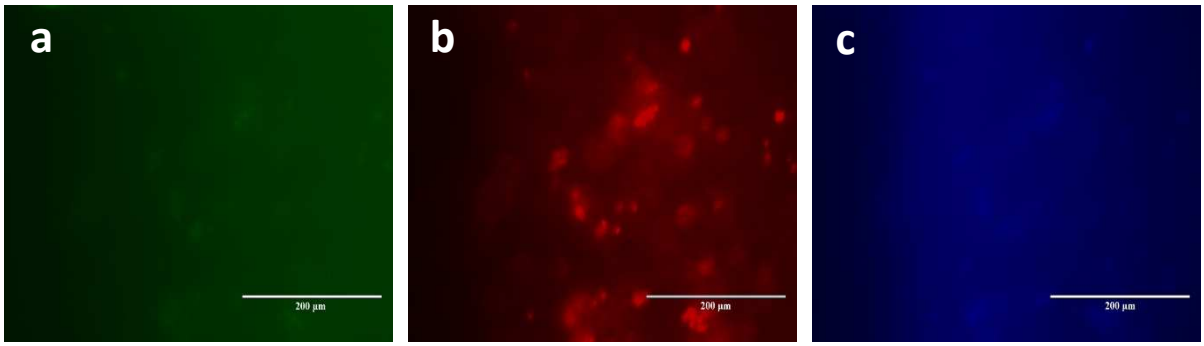

Figure A.4 *Immunofluorescence test on experiment 9 after 14 days: a) live cells marked in green by calcein-AM, b) dead cells marked in red by propidium iodide, c) total cells marked in blue by Hoechst 33258; 20X magnification.*

References

1. Liu Tsang, V. and S.N. Bhatia, *Three-dimensional tissue fabrication.* Advanced Drug Delivery Reviews, 2004. **56**(11): p. 1635-1647.
2. Aubin, H., et al., *Directed 3D cell alignment and elongation in microengineered hydrogels.* Biomaterials, 2010. **31**(27): p. 6941-6951.
3. Kaji, H., et al., *Engineering systems for the generation of patterned co-cultures for controlling cell–cell interactions.* Biochimica et Biophysica Acta (BBA) - General Subjects, 2011. **1810**(3): p. 239-250.
4. Tibbitt, M.W. and K.S. Anseth, *Hydrogels as extracellular matrix mimics for 3D cell culture.* Biotechnology and Bioengineering, 2009. **103**(4): p. 655-663.
5. Ustyugov, A.A., et al., *Development of 3D Cell Culture on Ultra-High Molecular Weight Polyethylene (UHMWPE) as the Basis of Cellular Matrix.* Biomedical Chemistry: Research and Methods, 2018. **1**(3).
6. Erler, J.T. and V.M. Weaver, *Three-dimensional context regulation of metastasis*. Clinical & Experimental Metastasis, 2009. **26**(1): p. 35-49.
7. Engler, A.J., et al., *Matrix Elasticity Directs Stem Cell Lineage Specification*. Cell, 2006. **126**(4): p. 677-689.
8. Chin, L.K., et al., *Mechanotransduction in cancer*. Current Opinion in Chemical Engineering, 2016. **11**: p. 77-84.
9. Ingber, D., *Mechanobiology and diseases of mechanotransduction*. Annals of medicine, 2003. **35**(8): p. 564-577.
10. Murphy, S.V. and A. Atala, *3D bioprinting of tissues and organs*. Nature biotechnology, 2014. **32**(8): p. 773-785.
11. Jungst, T., et al., *Strategies and molecular design criteria for 3D printable hydrogels*. Chemical Reviews, 2016. **116**(3): p. 1496-1539.
12. Hospodiuk, M., et al., *The bioink: A comprehensive review on bioprintable materials*. Biotechnology Advances, 2017. **35**(2): p. 217-239.
13. Geckil, H., *Engineering hydrogels as extracellular matrix mimics*. Nanomedicine, 2010. **5**: p. 469-484.
14. Dreifus, M., et al., *Intra-cameral lenses made of hydrocolloidal acrylates*. Ceskoslovenska oftalmologie, 1960. **16**: p. 154-159.

15. Hennink, W.E. and C.F. van Nostrum, *Novel crosslinking methods to design hydrogels.* Advanced Drug Delivery Reviews, 2002. **54**(1): p. 13-36.
16. Deligkaris, K., et al., *Hydrogel-based devices for biomedical applications.* Sensors and Actuators B: Chemical, 2010. **147**(2): p. 765-774.
17. Bajpai, A.K., et al., *Responsive Polymers in Biology and Technology.* Polymer Reviews, 2011. **51**(1): p. 53-97.
18. Fedorovich, N.E., et al., *Hydrogels as extracellular matrices for skeletal tissue engineering: state-of-the-art and novel application in organ printing*. Tissue Engineering, 2007. **13**(8): p. 1905–1925.
19. Schiele, N.R., et al., *Gelatin-based laser direct-write technique for the precise spatial patterning of cells*. Tissue Engineering Part C: Methods, 2011. **17**(3): p. 289–298.
20. Gauvin, R., et al., *Microfabrication of complex porous tissue engineering scaffolds using 3D projection stereolithography*. Biomaterials, 2012. **33**(15): p. 3824–3834.
21. Gruene, M., et al., *Laser printing of three-dimensional multicellular arrays for studies of cell–cell and cell–environment interactions.* Tissue Engineering Part C: Methods, 2011. **17**(10): p. 973–982.
22. Horváth, L., et al*., Engineering an in vitro air-blood barrier by 3D bioprinting*. Scientific Reports, 2015. **5**, 7974.
23. Zhu, J. and R.E. Marchant, *Design properties of hydrogel tissue-engineering scaffolds.* Expert Review of Medical Devices, 2011. **8**(5): p. 607-626.
24. Ara, T. and Y.A. DeClerck, *Mechanisms of invasion and metastasis in human neuroblastoma*. Cancer and Metastasis Reviews, 2006. **25**(4): p. 645-657.
25. Challagundla, K.B., et al., *Exosome-Mediated Transfer of microRNAs Within the Tumor Microenvironment and Neuroblastoma Resistance to Chemotherapy*. JNCI: Journal of the National Cancer Institute, 2015. **107**(7).
26. Pepelanova, I., et al., *Gelatin-Methacryloyl (GelMA) Hydrogels with Defined Degree of Functionalization as a Versatile Toolkit for 3D Cell Culture and Extrusion Bioprinting*. Bioengineering, 2018. **5**(3): p. 55-69.
27. Shirahama, H., et al., *Precise Tuning of Facile One-Pot Gelatin Methacryloyl (GelMA) Synthesis*. Scientific Reports, 2016. **6**, 31036.
28. Van Den Bulcke, A.I., et al., *Structural and Rheological Properties of Methacrylamide Modified Gelatin Hydrogels*. Biomacromolecules, 2000. **1**: p. 31-38.

29. Brigo, L., et al., *3D high-resolution two-photon crosslinked hydrogel structures for biological studies*. Acta Biomaterialia, 2017. **55**: p. 373-384.
30. Ahmed, E.M., *Hydrogel: Preparation, characterization, and applications: A review.* Journal of Advanced Research, 2015. **6**(2): p. 105-121.
31. Williams, C.G., et al., *Variable cytocompatibility of six cell lines with photoinitiators used for polymerizing hydrogels and cell encapsulation.* Biomaterials, 2005. **26**(11): p. 1211-1218.
32. Nichol, J.W., et al., *Cell-laden microengineered gelatin methacrylate hydrogels*. Biomaterials, 2010. **31**(21): p. 5536-5544.
33. Mironi-Harpaz, I., et al., *Photopolymerization of cell-encapsulating hydrogels: Crosslinking efficiency versus cytotoxicity.* Acta Biomaterialia, 2012. **8**(5): p. 1838-1848.
34. Lyubarev, A.E. and B.I. Kurganov, *Analysis of DSC data relating to proteins undergoing irreversible thermal denaturation*. Journal of Thermal Analysis and Calorimetry, 2000. **62**(1): p. 51-62.
35. Zhao, X., et al., *Photocrosslinkable gelatin hydrogel for epidermal tissue engineering*. Advanced Healthcare Materials, 2015. **5**(1): p. 108-118.
36. Di Giuseppe, M., et al., *Mechanical behaviour of alginate-gelatin hydrogels for 3D bioprinting*. Journal of the Mechanical Behavior of Biomedical Materials, 2018. **79**: p. 150-157.
37. Law, N., et al., *Characterisation of hyaluronic acid methylcellulose hydrogels for 3D bioprinting.* Journal of the Mechanical Behavior of Biomedical Materials, 2018. **77**: p. 389-399.
38. Zhou, S., et al., *Dead cell counts during serum cultivation are underestimated by the fluorescent live/dead assay.* Biotechnology Journal, 2011. **6**(5): p. 513-518.
39. Zhang, X., et al., *Exosomes in cancer: small particle, big player*. Journal of Hematology & Oncology, 2015. **8**, 83.

Websites:

https://advancedtissue.com/2019/01/what-is-hydrogel/ (Accessed 08/04/2019)

http://3dprintinggel.com/ (Accessed 08/04/2019)

https://wyss.harvard.edu/technology/3d-bioprinting/ (Accessed 08/04/2019)

https://www.thermofisher.com/it/en/home/references/gibco-cell-culture-basics/introduction-to-cell-culture.html (Accessed 11/05/2019)

https://www.labome.com/method/Cell-Culture-Media-A-Review.html (Accessed 11/05/2019)

https://www.researchgate.net/figure/Buerker-chamber-and-Fast-Read-102R-cell-count-method-The-Buerker-chamber-has-9-large_fig2_225084954 (Accessed 15/05/2019)

https://www.intechopen.com/books/hydrogels/enhancement-of-hydrogels-properties-for-biomedical-applications-latest-achievements (Accessed 26/08/2019)

https://www.sinobiological.com/principle-of-immunofluorescence.html (Accessed 19/09/2019)

https://courses.lumenlearning.com/microbiology/chapter/fluorescent-antibody-techniques/ (Accessed 19/09/2019)

https://www.thermofisher.com/it/en/home/life-science/cell-culture/mammalian-cell-culture/specialty-media/293-media.html (Accessed 22/10/2019)

https://www.sigmaaldrich.com/life-science/cell-culture/classical-media-salts/mem-media.html (Accessed 23/10/2019)